NATURALNESS IN F-SU(5)

A Dissertation

by

TRISTAN SHELTON LEGGETT

Submitted to the Office of Graduate and Professional Studies of
Texas A&M University
in partial fulfillment of the requirements for the degree of

DOCTOR OF PHILOSOPHY

Chair of Committee,	Dimitri Nanopoulos
Committee Members,	Bhaskar Dutta
	Stephen Fulling
	Christopher Pope
Head of Department,	George Welch

August 2014

Major Subject: Physics and Astronomy

ABSTRACT

We take a tour through modern high energy theory, beginning with the Standard Model, Supersymmetry, Supergravity, and Grand Unified Theories. We then review the constraints imposed by experiments on our model parameters and their derived quantities. We introduce Flipped-SU(5) and No Scale Supergravity as two of the building blocks of our model. We introduce $\mathcal{F}$-Theory and the $\mathcal{F}$-SU(5) model, including the motivations and experimental constraints. We intend to show that this model does not require an unnatural degree of fine tuning. First we shall use the tree level calculation of M_Z to obtain an estimate. The surprising results of the tree-level approximation will motivate generalization of the calculation. We find that the finetuning in this model is small, requiring accuracy in $M_{1/2}$ to at worst 10 %. We conclude that these results stem from the many experimental and theoretical constraints we impose on the model. We shall also introduce an M-theory derived model with mixed dilaton-moduli mediated supersymmetry breaking.

DEDICATION

To my family and friends, without whose support, encouragement, and occasional prodding this would not have been possible.

ACKNOWLEDGEMENTS

I would like to thank my advisor, Dimitri Nanopoulos, for his support, insights, and most of all, attitude. After every occasion of speaking with him, I felt a renewed drive to figure out how our universe works.

I would like to acknowledge Bhaskar Dutta and Christopher Pope for teaching me the foundations of high energy physics.

Tianjun Li was instrumental in the research presented here.

Special thanks are due to Sherree Kessler for administrative guidance in the production of this dissertation. Thanks also to the Mitchell Institute for the funding which helped me complete this research.

TABLE OF CONTENTS

Page

LIST OF FIGURES

FIGURE Page

LIST OF TABLES

TABLE Page

1. INTRODUCTION

1.1 Invitation

The recurring theme throughout this dissertation is one of simplicity. Occam's razor advises us to seek the simplest solution, other things being equal. The trend of unification in physics is one of utilizing one explanation for two or more phenomena. We will encounter numerous problems on our journey up the energy scale. We will find our problems multiplying. While we make only modest claims with regard to our work, we will find the the task of solving this multitude of problems is perhaps not as daunting as it might first appear. We shall find surprising alliances between disparate pieces of our theories. It is quite doubtful that Nature chose to implement every piece of the model as presented, but the existence of such a satisfactory model should give us hope that we do not need to rely on pure chance to explain the universe around us.

Throughout this dissertation we will use units where $\hbar = \mathrm{c} = 1$.

1.2 Selections from the Literature

Perhaps the most relevant papers to the specific model discussed in this dissertation are [1], [2], [3], [4], and [5]. One of the more accessible articles on F-theory model building is [6]. The author's introduction to supersymmetry was through [7]. Most of the experiments mentioned in 3 are referenced by their most up to date articles. Baer's recent work on finetuning is [8] and [9].

1.3 Preview

This dissertation is arranged roughly in the same manner that SuSpect [10] operates. We shall start from low energy theories and work our way to string theory,

then back down.

We shall begin with the fundamental building blocks in chapter 2. We introduce the Standard Model (SM) and take note of the gauge hierarchy problem. We suggest that SUSY will help us solve that problem but at the cost of doubling the world. We shall introduce supergravity (SUGRA) as a natural extension of global SUSY. We finish with an introduction to grand unified theories (GUTs) and some of the problems that previous models have encountered.

We cover the experimental constraints with an eye towards limiting the parameter space of our model in chapter 3. We introduce the astrophysical constraints from the cosmic microwave background as related to dark matter relic density. We shall discuss direct dark matter detection experiments and the tension between their results. Collider experiments are one of the more direct ways we may get data in our field, so we shall discuss the Large Hadron Collider experimental results of ATLAS and CMS, as well as the Brookhaven National Laboratory E-821 reults. As a subclass of collider experiments, we shall discuss rare decays, where we hope to obtain insight into beyond the SM physics by observing processes which would be heavily suppressed by the SM.

We introduce Flipped-SU(5) (F-SU(5)) as an example of a GUT theory in chapter 4. This GUT avoids many of the problems mentioned in chapter 1. We also introduce No-Scale SUGRA as a useful motivation for our boundary conditions and a way to have SUSY breaking without introducing a cosmological constant. These form two of the three major pillars upon which the $\mathcal{F}$-SU(5) model rests.

We cover the minimum amount of string theory necessary to motivate the remainder of the dissertation in chapter 5. From these points we begin our path back towards observable physics by considering the implications of $\mathcal{F}$-theory for F-SU(5). This provides our final pillar and we are able to begin building our model. We cover

the previous work done on the $\mathcal{F}$-SU(5) model as well as some extensions of that work done by the author.

In chapter 6 we investigate the finetuning required by the $\mathcal{F}$-SU(5) model. We find that the confluence of factors from previous chapters results in a very natural model. We compare these results with other phenomenological models.

In chapter 7 we present an alternative M-theory derived model. This three parameter model was unfortunately ruled out by not being able to satisfy both the WMAP relic dark matter density constraint and the LHC result for the lightest Higgs boson mass.

Finally, we draw our conclusions in chapter 8.

2. FOUNDATIONS

2.1 Standard Model of Particle Physics

We shall briefly review the SM in anticipation of introducing new particles with similar quantum numbers in chapter 5. **Leptons** are spin 1/2 fermions that are singlets under the strong nuclear force and exist in left-handed and right-handed chiralities. The right-handed leptons are also singlets under the weak nuclear force. The left-handed leptons are doublets under the weak nuclear force, pairing an electron-like field with a neutrino-like field for each generation. The lightest doublet is the electron and electron neutrino (e, ν_e), followed by the muon and muon neutrino (μ, ν_μ), and finally the heaviest is the tau and tau neutrino (τ, ν_τ). The right handed leptons similarly arrive in three generations, e, μ, and τ. The non-zero mass of neutrinos implies the existence of right handed chiralities, but as they are not charged under any known force except gravity, they have not yet been observed. **Quarks** are spin 1/2 fermions that are triplets under the strong nuclear force. Just as with leptons, they have two chiralities, the left-handed version interacting via the weak nuclear force. The three-left handed doublets are the up and down (u, d), strange and charm (s, c), and top and bottom (t, b). Tree-level Dirac masses are also forbidden by the chiral electroweak symmetry, so we require some mechanism to dynamically generate such masses.

The **gauge bosons** are spin 1 fields introduced into the Lagrangian to recover invariance under a local symmetry respected by the fermions. The gluons are the force carriers of the strong nuclear force and are introduced to make the Lagrangian invariant under a local SU(3) symmetry. Above the electroweak symmetry breaking (EWSB) scale, the W bosons are the force carriers of the weak nuclear force and are

introduced to provided invariance under a local SU(2) symmetry. Also above the EWSB scale, the B boson is the carrier of the hypercharge force. We observed a broken symmetry between the weak nuclear force and electromagnetism, this symmetry breaking results in a mixing between the neutral W and B bosons, the massive state is identified as the Z boson while the massless state is identified with the photon. The only way to break this symmetry without spoiling the renormalizability of the theory is by breaking it spontaneously, i.e. allowing the Hamiltonian to remain invariant but the specific state to violate the symmetry. This was introduced into particle physics by Peter Higgs.

The Higgs mechanism introduces a complex spin 0 weak doublet (the **Higgs** field) which acquires a nonzero vacuum expectation value (vev) which will be denoted as v. We may rotate this vev such that it belongs to a single real component of our Higgs field. Then the other three degrees of freedom are known as Goldstone bosons. Each Goldstone boson may be absorbed by one of the massive gauge bosons to give three degrees of freedom to that field, effectively giving it mass. At the same time, through the Yukawa coupling of the Higgs field to SM fermions, terms of the form $Y_{h\psi\psi}h\psi\psi$ will acquire effective mass terms as we replace the Higgs field with its vev.

If we consider the one-loop correction to the Higgs mass, we immediately find the serious **gauge hierarchy problem**.

$$\delta M_h \propto \int_0^\Lambda \frac{d^4k}{k^2} \propto \Lambda^2 \tag{2.1}$$

Λ is our high energy cutoff, where the SM is no longer valid as an effective theory. If we are to have EWSB, we require M_h to not be too much larger than the electroweak scale ($\lesssim$ 1 TeV). At this point, without other alternatives, we would expect Λ to be approximately the Planck scale. This would then correspond to a

Planck scale addition to the Higgs mass, immediately wiping out EWSB. Of the proposals to avoid this problem, the most successful and only one we will consider is supersymmetry.

2.2 Supersymmetry

Unlike the gauge symmetries introduced previously supersymmetry (SUSY) mixes bosonic and fermionic representations of the Lorentz group. Thus, SUSY predicts the existance of a particle with the same quantum numbers as the electron, except the spin of the selectron is 0. Because all other quantum numbers are the same, we will often be able to substitute a sparticle for a particle in a Feynman diagram. For example, in the calculation of the quantum corrections to the Higgs mass for every diagram containing a top quark there would be a diagram that instead contains a stop squark of similar amplitude. If we consider a loop with a top quark, the anticommutivity of the fermionic quark will give an opposite sign to the amplitude compared to the commuting squark. Therefore these two diagrams will destructively interfere. This will eliminate the quadratic divergence that we found above. This is not a satisfactory solution, though, because we do not observe equal mass particle-sparticle pairs. If we may softly break supersymmetry, we may retain the cancellation of the quadratic divergences while providing for a mass difference within supersymmetric multiplet. At this point, we must consider such soft-SUSY breaking mass parameters to be put in by hand. We will find motivation for such parameters in the next section and when we consider string theory.

The Minimal Supersymmetric Standard Model (MSSM) is a useful basis of comparison and a general phenomenological starting point for many SUSY models. It posits the existance of the SM fields, their supersymmetry partners, and two Higgs doublets. Because it makes no assumptions about the relations between the soft

breaking masses for each field, there are a plethora of free parameters.

2.3 Supergravity

We have found tremendously useful and interesting theories by promoting U(1), SU(2), and SU(3) to local symmetries. If we consider local supersymmetry, we find ourselves surprised by an old friend. Upon allowing the infinitesimal fermionic parameter ϵ to vary, we shall need a spin 3/2 field to cancel the contribution from the term proportional to $\partial_\mu \epsilon(x)$. This Rarita-Schwinger field will require a partner under supersymmetry with spin 2. We may identify these fields as the gravitino and graviton, respectively. We have found that local supersymmetry immediately implies supergravity (SUGRA). The introduction of fields with spin higher than 1 spoils our efforts at renormalization. There is a possible exception with $\mathcal{N} = 8$ SUGRA [11], but while interesting, that is not the subject of this work. This lack of renormalizability does not prevent us from considering SUGRA as an effective field theory, in particular in deriving the soft SUSY breaking masses or utilizing its framework for the running of the renormalization group equations (RGEs). The many SUGRA models that are low energy limits of string theory also provide a useful framework for dealing with string phenomenology.

Supposing that the SUSY soft breaking masses end up being close enough to the weak scale to not generate problems, the Higgs mass mixing paramter μ is a SUSY conserving quantity. There is nothing forbidding it from being at the Planck scale as opposed to the weak scale. This is known as the μ **problem**. One particular model that will introduce many concepts that we shall need in later chapters is minimal supergravity (mSUGRA). This model assumes universal soft terms for the gauginos (SUSY partners of the gauge bosons), sfermions (partners of the SM fermions), and trilinear couplings. These parameters are $M_{1/2}$, M_0, and A_0 respectively. The model

also requires the value of $\tan\beta = v_u/v_d$ at the EWSB scale and the sign of the Higgs mass mixing parameter, $sign(\mu)$. mSUGRA unfortunately did not fare well under the onslaught of experimental evidence unleashed by the Large Hadron Collider.

2.4 Grand Unified Theories

The considerable experimental success of the Glashow Salam Weinberg electroweak unification gives inspiration for unification of all the forces. If we simply consider the running of the SM RGEs with the known low energy boundary conditions, we find the the coupling strengths approach each other around 10^{15} GeV. If we instead consider the MSSM with some general assumptions about the SUSY sector, we find that the coupling strengths actually meet around 10^{16} GeV. With this as an indicator that we are on the right path, we may now look for groups into which we may fit the SM.

The smallest group that can accommodate the SM is SU(5). Among the unexpected surprises, we find a natural explanation for the quantization of electric charge from GUTs. The simplest example demonstrating this is the Georgi-Glashow SU(5) model. By placing a triplet of (conjugate) down quarks in the same representation as the left handed leptons, the requirement that the sum of the electric charges of this multiplet be zero explains why the quarks have 1/3 or 2/3 of the charge of the electrons. For comparison with the particle content of Flipped SU(5) presented later, the Georgi-Glashow model has [12]:

$$\bar{\mathbf{5}} = \begin{pmatrix} d^1 \\ d^2 \\ d^3 \\ e^C \\ \nu^C \end{pmatrix}_R \quad ; \quad \mathbf{10} = \begin{pmatrix} 0 & u_3^C & -u_2^C & -u^1 & -d^1 \\ -u_3^C & 0 & u_1^C & -u^2 & -d^2 \\ u_2^C & -u_1^C & 0 & -u^3 & -d^3 \\ u^1 & u^2 & u^3 & 0 & -e^+ \\ d^1 & d^2 & d^3 & e^+ & 0 \end{pmatrix}_L \tag{2.2}$$

In addition, we shall have a GUT-breaking Higgs $\Sigma = \mathbf{24}$ and two electroweak-breaking Higgs, $h = \mathbf{5}$. h must contain color triplets in order to complete the representation, which we will see below cause issues with proton decay.

From this same starting point, allowing quark-lepton mixing also introduces the possibility of baryon number and lepton number violation, providing one of the Sakharov conditions for baryogensis.

A less flashy, but important prediction is the unification of Yukawa couplings at the GUT scale. A significant reduction in parameters is always welcome in comparison to the plethora we found with the MSSM.

Unfortunately, the introduction of SUSY into SU(5) allows effective dimension 5 operators to mediate proton decay through contraction of two sfermions with two fermions mediated by Higgs fields [13], for example, $\frac{-\epsilon_{\alpha\beta\gamma}}{2M_T} C_{5L}^{ijkl} Q_{i\alpha} Q_{j\beta} Q_{k\gamma} L_l$ and $\frac{-\epsilon_{\alpha\beta\gamma}}{2M_T} C_{5R}^{ijkl} U_{i\alpha}^C D_{j\beta}^C U_{k\gamma}^C E_l^C$. Where Greek indicies are for color, Latin are for family, M_T is the mass of the mediating color triplet, and the C's are constant tensors in family-space. The amplitude is then inversely proportional to M_T, and so the proton lifetime is proportional to M_T^2. If we require consistency with known bounds on the proton lifetime, we obtain $M_T \sim 4.4 * 10^{17}$ GeV (with broad assumptions regarding a lattice calculation coefficient, sfermion masses, and $\tan\beta$). If we then cannot forbid mixing between this color triplet and our EWSB Higgs (as for example occurs in the Georgi-Glashow model), then we spoil radiative EWSB. As we will see later,

$\mathcal{F}$-SU(5) has all of the good parts of GUTs, as inherited from a true GUT (i.e. E_8) under string theory, while avoiding the problems of simpler GUTs.

3. EXPERIMENTAL CONSTRAINTS

The early and middle of the twentieth century saw a plethora of particle physics data. This led to the formulation of the SM and its numerous successes. However, we have seen a slowing of progress, with the discovery of the Higgs coming twenty years after the discovery of the top quark. Our sources of data come from three main sources. Astrophysical, including both looking at the very early universe and using astronomical scales to see the effects of dark matter. Collider physics is perhaps the most direct source of data, though it can be plagued by large backgrounds and overall expense. Precision measurements of the anomalous magnetic moment of the muon and rare decays are frequently measured at colliders to provide very stringent constraints on possible SUSY contributions.

Dark matter was originally proposed to explain the unexpected observations of galactic rotation curves in the middle of the twentieth century. From WMAP, we know that approximately 27 % of the energy density in the universe is dark matter, compared to approximately 5 % for visible matter, and the remaining 72 % of dark energy. The Planck satellite [14] reported the cold dark matter density Ωh^2 to be 0.1199 ± 0.0027. Frequently in SUSY models, including the $\mathcal{F}$-SU(5) model discussed beginning in chapter 5, a natural candidate for dark matter is provided by the lightest supersymmetric particle (LSP). In order for this particle to be a dark matter candidate, it must be neutral under the strong and electromagnetic forces, so it only interacts weakly and gravitationally. Because of the weak interaction and the matter-like (as opposed to radiation-like) state, the particle candidates for dark matter are called Weakly Interacting Massive Particles (WIMPs). The scenario we will favor has the LSP as a mixture of the bino, wino, and higgsinos, though the

gravitino and sneutrinos are not ruled out as dark matter candidates.

Regardless of whether WIMPs are the LSP, there are a variety of experiments that seek to observe the interaction of a WIMP with baryonic matter. These **direct detection** experiments generally work by having a large detector with enough shielding to strongly attenuate all except for the most weakly interacting particles. Based upon the recoil of a nucleus upon interaction with a WIMP, a signal can then be extracted. The frequency of such collisions together with knowledge of how much material is in the detector allows a cross section to be estimated. The second phase of the Cryogenic Dark Matter Search experiment (CDMS II) claims a signal plus background hypothesis is more likely than the pure background hypothesis [15]. This result does not reach discovery level significance, but the favored WIMP mass is 8.6 GeV and the cross section is $1.9 \times 10^{-41} cm^2$. The XENON100 experiment claims to have found no signal, with a lowest exclusion cross section of $2.0 \times 10^{-45} cm^2$ for a WIMP mass at 55 GeV [16]. The Large Underground Xenon (LUX) experiment currently reports no detection of WIMPs, setting 90 % confidence level on the spin-independent cross section between WIMPs and nucleons [17]. This limit depends on the WIMP mass, but the smallest cross section is for a 33 GeV WIMP at $7.6 \times 10^{-46} cm^2$. There is obviously some tension between these experiments, we shall take the exclusion results for this work.

The Large Area Telescope on the Fermi Gamma Ray Space Telescope (Fermi-LAT) [18], [19] has found a possible signal with two interpretations based upon approximately fifty photons. If the signal is the result of internal bremsstrahlung of a dark matter particle, then the particle would have mass of $149 \pm 4^{+8}_{-15}$ GeV with an annihilation rate of $\langle \sigma v \rangle_{\chi\chi \to \bar{f} f \gamma} = (6.2 \pm 1.5^{+0.9}_{-1.4}) \times 10^{-27} cm^2 s^{-1}$. This signal could also fit dark matter annihilation into photon pairs with dark matter mass $129.8 \pm 2.4^{+7}_{-13}$ and $\langle \sigma v \rangle_{\chi\chi \to \gamma\gamma} = (1.27 \pm 0.32^{+0.18}_{-0.28}) \times 10^{-27} cm^2 s^{-1}$.

The MSSM requires 2 complex Higgs doublets, resulting in a total of eight degrees of freedom. Three of these are absorbed to give the W and Z gauge bosons mass. That leaves us with 5 Higgs-like particles remaining, two neutral scalars, a neutral pseudoscalar, and two charged scalars. The tree-level lightest Higgs mass is less than M_Z, however, given that the concern about radiative corrections is what fundamentally motivated much of this work, we would be unsurprised to find that they are significant enough to push M_h above M_Z. Until mid 2012, the Large Electron Positron Collider exclusion limit of 114 GeV was the only lower limit available. The SUSY preferred region between 114 GeV and 135 GeV represented only the lower end of the SM allowed limit. Two experiments at the Large Hadron Collider (LHC) announced the discovery of the lightest Higgs in July 2012. The mass was measured as 126.5 GeV from ATLAS, [20] and 125.3 GeV from CMS [21].

Historically, one of the major successes of quantum field theory was the calculation of the anomalous magnetic moment of the electron. Because the muon is two hundred times heavier than the electron, it is considerably more sensitive to loop corrections from heavy particles. In particular, the addition of SUSY particles provides corrections well within experimental reach. While the single measurement is not sufficient to advance our knowledge of SUSY particles, it is sufficient to eliminate swaths of parameter space. The E821 experiment at Brookhaven National Laboratory gives us an anomalous magnetic moment of the muon of $\Delta a_\mu < 11659208(6) \times 10^{-10}$. The positive value indicates a preference for the SUSY μ term to be positive [22].

Rare decay processes have the capability to provide insight into beyond the SM physics. The rare decay $b \to X_s\gamma$ occurs via a flavor changing neutral current, and is thus highly suppressed in the SM. Moving chronologically, the CLEO collaboration [23] measured $\mathcal{B}r(b \to s\gamma)$ to be $(0.43 \pm 0.27^{+0.18}_{-0.10}) \times 10^{-4}$. This was followed by BaBar [24] in 2008 with $\mathcal{B}r(B \to X_s\gamma) = (3.66 \pm 0.85_{stat} \pm 0.60_{sys}) \times 10^{-4}$. The Belle

collaboration [25] in 2009 measured $\mathcal{B}r(B \to X_s\gamma) = (3.45 \pm 0.15_{stat} \pm 0.40_{sys}) \times 10^{-4}$.

In 2013 two LHC experiments measured $\mathcal{B}r(B_s^0 \to \mu^+\mu^-)$ and $\mathcal{B}r(B^0 \to \mu^+\mu^-)$. LHCb measured an excess at 4.0 standard deviations relative to the SM in $B_S^0 \to \mu^+\mu^-$ with a branching ratio of $(2.9^{+1.1}_{-1.0}) \times 10^{-9}$ [26] and an upper limit of $\mathcal{B}r(B^0 \to \mu^+\mu^-)$ ¡ 7.4×10^{-10}. CMS measured an excess at 4.3 standard deviations relative to the standard of $\mathcal{B}r(B_s^0 \to \mu^+\mu^-) = (3.0^{+1.0}_{-0.9}) \times 10^{-9}$. The upper limit of $\mathcal{B}r(B^0 \to \mu^+\mu^-)$ at 95% confidence level was measured at 1.1×10^{-9}.

The experimental constraints presented here are useful for narrowing the parameter space used by any particular model. In addition, the lack of a SUSY signal at the LHC so far is useful in being able to rule out points in parameter space once their spectrum has been calculated. In particular, we note a peculiarity in $\mathcal{F}$-SU(5) in that it tends to show a small increase in events with a high number of jets [27].

4. FLIPPED-SU(5)

4.1 F-SU(5)

We saw above that Georgi-Glashow's SU(5) grand unified theory is not experimentally viable. The original motivation for Flipped-SU(5) was to suppress proton decay and obtain better values for $\sin^2\theta_W$ [28]. A minimal fix that we may apply to this model is by reusing the lesson we learned with the Glashow-Weinberg-Salam model of electroweak unification, i.e. add in a U(1) symmetry. In addition, we will shuffle the fields in the representations to end up with:

$$\bar{f} = (\mathbf{5}, -3) = \begin{pmatrix} u_1^C \\ u_2^C \\ u_3^C \\ \nu \\ e \end{pmatrix}_L \quad ; \quad F = (\mathbf{10}, 1) = \begin{pmatrix} 0 & d_3^C & -d_2^C & d^1 & u^1 \\ -d_3^C & 0 & d_1^C & d^2 & u^2 \\ d_2^C & -d_1^C & 0 & d^3 & u^3 \\ -d^1 & -d^2 & -d^3 & 0 & \nu^C \\ -u^1 & -u^2 & -u^3 & -\nu^C & 0 \end{pmatrix}_L .$$

in addition to right handed electron singlet, $l^C = (\mathbf{1}, 5)$. Our Higgs multiplets, with an abbreviated notation, are given by:

$$H = (\mathbf{10}, 1) = (Q_H, d_H^C, \nu_H^C) \quad ; \quad \bar{H} \quad ; \quad h = (\mathbf{5}, -2) = (h_2, h_3) \quad ; \quad \bar{h}.$$

The GUT superpotential gives us

$$\lambda_{HHh} HHh + \lambda_{\bar{H}\bar{H}\bar{h}} \bar{H}\bar{H}\bar{h} + \lambda_{F\bar{H}\Phi} F\bar{H}\Phi + \mu h\bar{h} \in W_{GUT}$$

The first two terms give us non-mixing masses for the color triplet Higgs terms h_3 and $\bar{h}_3$. This allows the electroweak Higgs h_2 to remain light in accord with EWSB.

These small changes end up suppressing proton decay to experimentally viable rates, provide doublet-triplet Higgs splitting, and give a natural see-saw mechanism to generate small left handed neutrino masses and large right handed neutrino masses.

The orders of magnitude difference between $M_{GUT} \sim 10^{16}$ GeV and the string or Planck scale is known as the **little hierarchy problem** (Baer, among others, sometimes refers to the cancellation between TeV scale SUSY parameters to yield M_Z as the little hierarchy problem). This separation and the exclusion of gravity from the SM suggests that true unification would occur at the string scale. F-SU(5) has a natural separation between the partial unification of SU(3) and SU(2) at M_{32} and the final unification at the string scale, M_F, as shown in figure 4.1.

4.2 No Scale Supergravity

The primary motivation of No Scale Supergravity (NSS) is a natural vanishing of the cosmological constant while maintaining broken supersymmetry.

For example, with a single chiral superfield we have:

$$V = e^G(G_T G^{-1}_{T\bar{T}} G_{\bar{T}} - 3)$$

where

$$G = K/M^2_{Pl} + \log|W|^2 \tag{4.1}$$

This is accomplished through the use of a Kähler potential depdending on the moduli T of the form:

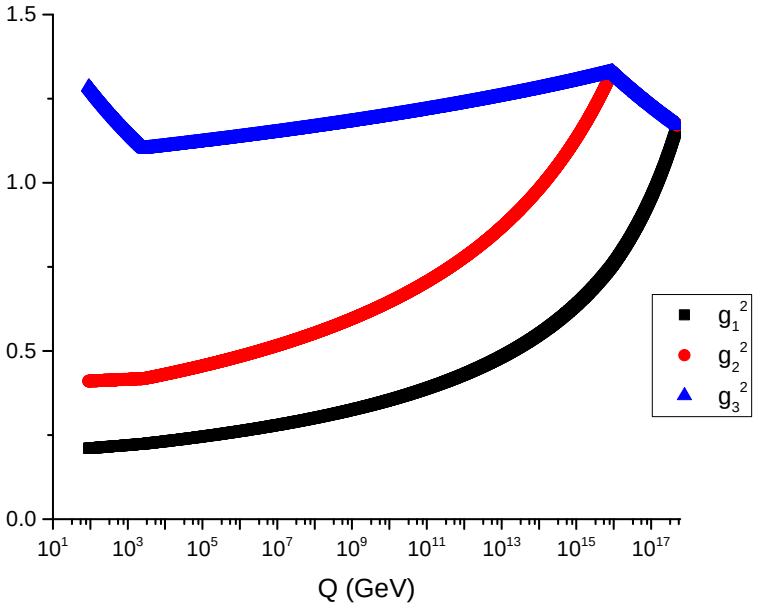

Figure 4.1: The partial unification of SU(3) and SU(2) at M_{32} and final unification at M_F.

$$K = 3\log(T + \bar{T}) + ... \tag{4.2}$$

In addition, a model satisfying the NSS conditions will also have flat directions so that the gravitino mass is free and $\mathrm{Str}\mathcal{M}^2 = 0$. The last condition is necessary to maintain a gravitino mass above the weak scale and below the Planck scale. This Kähler potential also gives us the boundary conditions that will prove instrumental in the naturalness of our model, $M_0 = A_0 = B_\mu = 0$.

5. F-THEORY AND APPLICATIONS

5.1 String and $\mathcal{F}$-Theory

String theory is the only known framework for both quantizing gravity and unifying gravity with other forces. The appearance of the spin 2 graviton is what motivated the shift from considering string theory as a theory of the strong force to a quantum theory of gravity. For a basic supersymmetric theory, we may obtain a 10 dimensional space-time. Because we have observed only four space-time dimensions, we surmise that the remaining dimensions are compactified, in particular into a three complex dimensional Calabi-Yau manifold. Of the many directions to pursue from this, we shall be content with citing this manifold as the origin of our moduli fields, which will ultimately generate our model parameters. Five major distinct forms of string theory are known, and these are related to each other by dualities, I, IIA, IIB, heterotic SO(32), and heterotic $E_8 \times E_8$. M-theory was originally constructed as a strongly coupled limit of heterotic $E8 \times E8$ in eleven dimensions. We shall consider an M-theory model in chapter 7. In particular we will be concerned with a strongly coupled type IIB theory with a varying axion-dilaton, known as $\mathcal{F}$-theory.

We may start with a twelve dimensional space, two dimensions to parameterize the axion-dilaton, six dimensions for the internal Calabi-Yau manifold, and four for space-time. To eventually get the SM, we would like to have a space-time filling 7-brane which will wrap a subspace S of the Calabi-Yau manifold B. Our gauge theory will live on this brane, our matter fields will live at the intersection of this brane and another, and our Yukawa couplings will come from the triple intersection of three of these branes [6].

We obtain a gauge theory by identifying the way in which the axion-dilaton

becomes singular near the 7-brane with a Lie group.

$$\frac{1}{g_{YM}^2} \sim M_{Pl} \frac{Vol_4(S)}{\sqrt{Vol_6(B)}} \tag{5.1}$$

This section is primarily concerned with providing a basic intuition for where the $\mathcal{F}$-SU(5) model comes from in the ultraviolet limit.

5.2 $\mathcal{F}$-SU(5)

With string theory, and particularly the $\mathcal{F}$-theory construction provided above, we now have completed our collection of tools required to build a natural and realistic model.

5.2.1 Flippons and F-Theory Derivation

$\mathcal{F}$-theory provides a convenient method for the introduction of vector-like fermions (flippons). These flippons may be introduced on the same 7-brane that our gauge fields inhabit. The gravity mediated supersymmetry breaking structure of No Scale Supergravity provides a global framework within which we may calculate the Kähler potential for the SM fermions and Higgs fields.

We require that the set of flippons we introduce satisfy $\Delta b_1 < \Delta b_2 = \Delta b_3$ and must not introduce a Landau pole in the strong coupling constant. Thus we have five possible sets [29]:

$$
\begin{aligned}
&Z1 : XF, \bar{XF}, \\
&Z2 : XF, \bar{XF}, Xl, \bar{X}l \\
&Z3 : XF, \bar{XF}, Xf, \bar{X}f \\
&Z4 : XF, \bar{XF}, Xl, \bar{X}l, Xh, \bar{X}h \\
&Z5 : XF, \bar{XF}, Xh, \bar{X}h
\end{aligned}
\tag{5.2}
$$

where under $SU(5) \times U(1)_X$

$$
\begin{aligned}
&XF = (\mathbf{10}, \mathbf{1}), \bar{XF} = (\bar{\mathbf{10}}, -\mathbf{1}) \\
&Xf = (\mathbf{5}, \mathbf{3}), \bar{X}f = (\bar{\mathbf{5}}, -\mathbf{3}) \\
&Xl = (\mathbf{1}, -\mathbf{5}), \bar{X}l = (\mathbf{1}, \mathbf{5}) \\
&Xh = (\mathbf{5}, -\mathbf{2}), \bar{X}h = (\bar{\mathbf{5}}, \mathbf{2})
\end{aligned}
\tag{5.3}
$$

These decompose under the SM as follows:

$$
\begin{aligned}
&XF = (XQ, XD^C, XN^C) \\
&Xf = (XU, XL^C) \\
&Xl = XE \\
&Xh = (XD, XL)
\end{aligned}
\tag{5.4}
$$

and similarly for the conjugates.

The representations of the SM (and hence the names of each field) for these are:

$$\begin{aligned} XQ &= (\mathbf{3}, \mathbf{2}, \frac{\mathbf{1}}{\mathbf{6}}) \\ XU &= (\mathbf{3}, \mathbf{1}, \frac{\mathbf{2}}{\mathbf{3}}) \\ XD &= (\mathbf{3}, \mathbf{1}, \frac{\mathbf{-1}}{\mathbf{3}}) \\ XL &= (\mathbf{1}, \mathbf{2}, \frac{\mathbf{-1}}{\mathbf{2}}) \\ XE &= (\mathbf{1}, \mathbf{1}, \mathbf{-1}) \\ XN &= (\mathbf{1}, \mathbf{1}, \mathbf{0}) \end{aligned} \tag{5.5}$$

and again, similarly for the conjugates.

We shall deal exclusively with the Z2 set.

5.2.2 No Scale SUGRA

With the final unification at the string scale, we now have a justification for the No Scale SUGRA boundary conditions $M_0 = A_0 = B_\mu = 0$.

These flippons are charged under the SM and so will modify the RGEs as written in common codes, e.g. SuSpect [10]. Additionally, the extension of the RGEs over the phase transition between the SM and F-SU(5) requires modifications that respect the high energy symmetry. As a first approximation we include the flippon modifications to the RGEs at two loop for the gauge coupling strengths, one loop for the SM fermion Yukawa couplings, μ term, and soft SUSY breaking terms.

Using the NSS boundary conditions, we can minimize the potential as a function of $M_{1/2}$, and thereby dynamically determine $M_{1/2}$. This condition $dV_{min}/dM_{1/2} = 0$

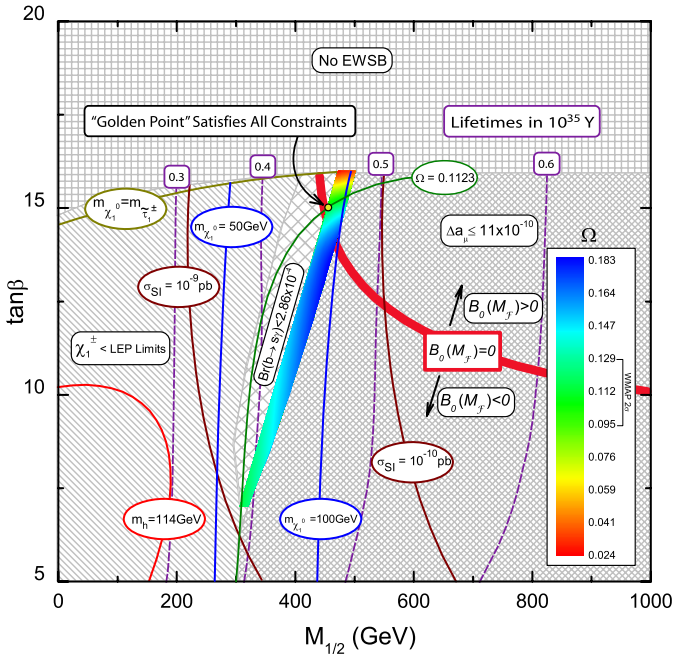

Figure 5.1: An initial application of the experimental constraints covered in chapter 3. M_V was restricted to 1 TeV, the LHC Higgs mass measurements had not been released yet, and the Ωh^2 data is taken from WMAP 7. This figure was taken from [1].

is referred to in the literature as the Super No Scale condition. From a high energy scale perspective, we can think of this as the stabilization of the moduli that generate the F-term giving $M_{3/2}$ and ultimately $M_{1/2}$.

5.2.3 One Parameter Model

We initially take four free parameters in this implementation of our model. $M_{1/2}$, M_V, $\tan\beta$, and M_{top} give us a four dimensional parameter space. After applying the experimental constraints listed in 3, some of which are shown in 5.1, and enforcing the No-Scale SUGRA boundary conditions (namely $B_\mu(M_F)$=0), we are left with an essentially one dimensional subspace.

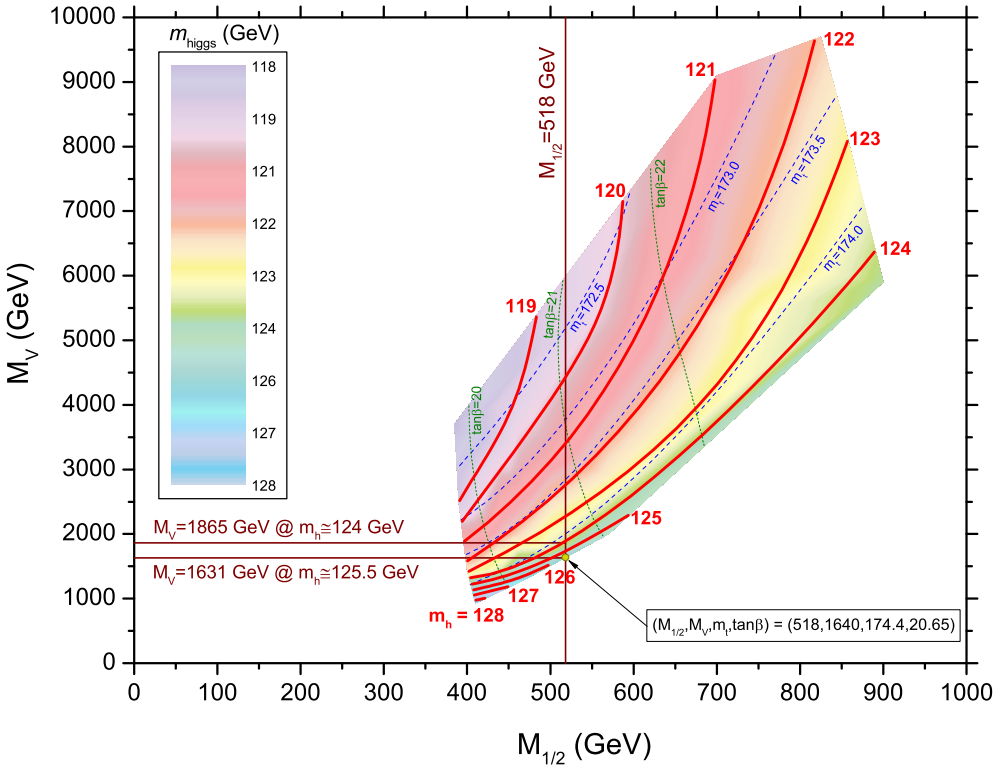

Figure 5.2: Upon measurement of the lightest Higgs mass at the LHC, flippon contributions to the same were considered more closely. Using a similar set of benchmark points as in the previous figure, but allowing M_V to increase from 1 TeV, we find that this model obtains heavier Higgs masses than are normally favored. The top quark mass was also allowed to vary in an effort to obtain more of a parameter space than the Golden Point as mentioned in [1]. This figure was taken from [2].

Further refinements on the parameter space are displayed in figure 5.2.

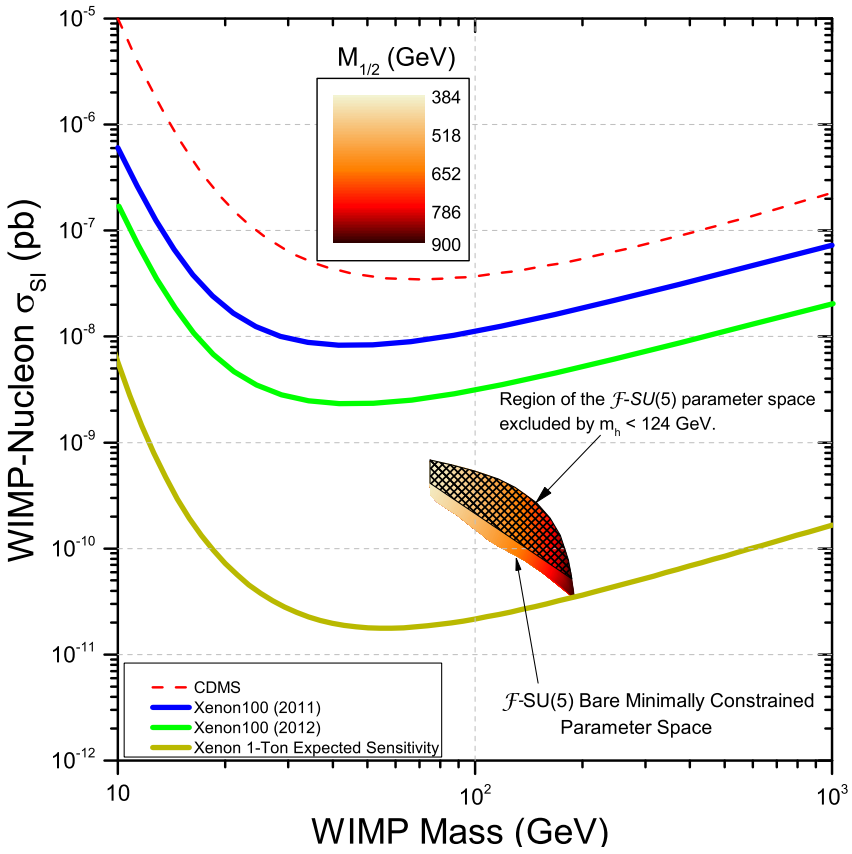

Figure 5.3: The announcement of direct dark matter detection experiment results over the last few years motivated an analysis of how $\mathcal{F}$-SU(5) would fare in future experiments. As shown, this model is in stark disagreement with the low mass WIMPs as reported by several experiments, but is within the reach of the future incarnation of the XENON experiment. This figure was taken from [3].

The imminent availability of experimental verification of the $\mathcal{F}$-SU(5) model is demonstrated in figure 5.3.

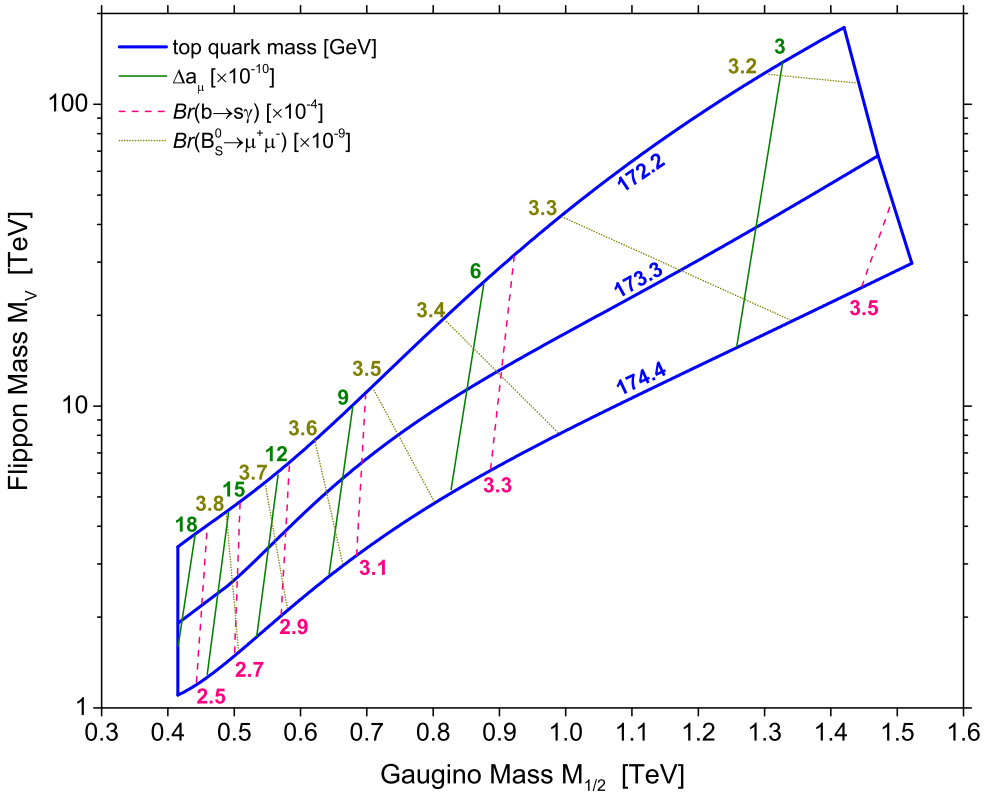

Figure 5.4: A larger wedge was obtained by increasing the range for M_V while floating the top quark mass. The range of $\tan\beta$ was unaffected. The announcement of rare decay results from CMS and LHCb motivated an examination of how those limits affected the parameter space. Limits from the anomalous magnetic moment of the muon were also included. This figure was taken from [4].

Variation within allowed values of the rare decays and anomalous magnetic moment of the muon are displayed in figure 5.4.

The post-Higgs mass benchmark points with $M_{top} = 172.2$ GeV we are using are described in Table 5.1 along with a small sample of the spectrum.

$M_{1/2}$	$\tan\beta$	M_V	$M_{\tilde{\chi}_1^0}$	M_h	$M_{\tilde{t}_1}$	$M_{\tilde{t}_2}$	$M_{\tilde{g}}$
415	20.00	2800	80.3	119.4	436	803	579
500	21.04	4705	100.6	119.8	541	925	695
590	21.88	7740	122.8	120.2	649	1052	819
600	21.95	8076	125.2	120.2	660	1067	833
700	22.61	12324	150.3	120.8	777	1210	969
800	23.10	17743	175.9	121.3	891	1353	1106
889	23.49	25300	199.6	121.7	992	1478	1229
1000	23.90	41673	230.6	122.2	1115	1630	1386
1100	24.24	68515	260.0	122.5	1225	1763	1531
1230	24.54	100500	296.7	123.0	1368	1943	1713
1300	24.69	127663	317.4	123.2	1444	2038	1813
1405	24.85	171066	348.1	123.5	1558	2182	1962
1420	24.88	179243	352.6	123.6	1575	2202	1984

Table 5.1: Parameters and select masses for $M_{top} = 172.2$ GeV. All masses are in GeV.

The more central values of $M_{top} = 173.3$ GeV have their benchmark points and spectrum described in table 5.2.

$M_{1/2}$	$\tan\beta$	M_V	$M_{\tilde{\chi}_1^0}$	M_h	$M_{\tilde{t}_1}$	$M_{\tilde{t}_2}$	$M_{\tilde{g}}$
415	19.75	1811	78.6	121.7	433	814	574
432	20.00	1986	82.5	121.7	454	838	597
446	20.34	2360	85.9	121.2	472	856	617
479	20.58	2598	93.4	121.6	512	906	661
501	20.82	2844	98.4	121.7	540	939	690
524	21.03	3138	103.8	121.7	568	973	720
555	21.29	3537	111.0	121.9	605	1019	762
583	21.50	3945	117.6	121.9	638	1060	799
614	21.75	4618	125.2	122.0	675	1104	841
650	22.02	5387	134.0	122.1	717	1156	890
655	22.04	5500	135.2	122.1	723	1163	897
686	22.25	6268	142.9	122.1	759	1207	938
724	22.56	7015	151.9	122.3	804	1263	989
750	22.63	8095	158.9	122.4	833	1299	1025
788	22.80	9227	168.5	122.6	876	1354	1076
825	22.98	10498	177.8	122.7	918	1407	1127
867	23.15	11831	188.4	122.9	966	1468	1183
901	23.30	13166	197.2	123.0	1004	1516	1229
931	23.42	14384	204.9	123.2	1038	1559	1269
966	23.53	15910	214.0	123.3	1077	1609	1316
1000	23.67	17356	222.7	123.4	1115	1658	1362
1080	23.91	22100	244.1	123.7	1203	1770	1470
1200	24.26	30830	276.4	124.1	1335	1938	1633
1300	24.51	39974	303.9	124.4	1444	2077	1770
1387	24.68	52500	328.8	124.7	1538	2196	1892
1471	24.82	67690	353.2	124.9	1628	2310	2010

Table 5.2: Parameters and select masses for $M_{top} = 173.3$

$M_{1/2}$	$\tan\beta$	M_V	$M_{\tilde{\chi}_1^0}$	M_h	$M_{\tilde{t}_1}$	$M_{\tilde{t}_2}$	$M_{\tilde{g}}$
415	19.46	1080	76.6	126.7	429	827	568
450	19.89	1200	84.1	126.9	474	881	614
518	20.62	1640	99.4	125.8	558	982	704
550	20.96	1950	106.9	125.2	597	1028	747
570	21.08	2050	111.3	125.3	621	1059	773
650	21.69	2750	130.0	125.0	716	1177	878
675	21.85	2950	135.7	125.0	746	1215	910
700	22.02	3350	142.0	124.7	775	1250	944
725	22.23	3750	148.1	124.5	804	1285	977
729	22.24	3815	149.0	124.6	809	1292	983
775	22.53	4800	160.6	124.4	861	1356	1047
825	22.68	5300	172.7	124.6	918	1431	1111
850	22.78	5500	178.6	124.8	947	1469	1143
875	22.86	5700	184.4	124.9	975	1507	1176
900	22.97	5880	190.3	126.5	1004	1544	1207
950	23.18	7010	203.1	125.0	1060	1615	1275
990	23.34	8044	213.5	125.1	1104	1672	1328
1090	23.67	10200	238.8	125.3	1216	1816	1460
1170	23.93	13290	260.3	125.4	1303	1927	1569
1295	24.23	17233	292.9	125.8	1440	2106	1734
1387	24.45	21020	317.4	126.1	1540	2235	1856
1500	24.67	27636	348.5	126.3	1661	2391	2009
1522	24.73	30271	355.2	126.3	1684	2419	2041

Table 5.3: Parameters and select masses for $M_{top} = 174.4$

For completeness, the benchmark points and spectra with $M_{top} = 174.4$ GeV are included in table 5.3.

We also wish to calculate the correction the flippons give to the lightest Higgs mass. As a first approximation, we follow [30] with:

$$
\begin{aligned}
\Delta m_h^2 &= -\frac{3}{8\pi^2} M_Z^2 \cos^2 2\beta (\hat{Y}_{xu}^2 + \hat{Y}_{xd}^2) t_V + \frac{3v^2}{4\pi^2} \times \{ \hat{Y}_{xu}^4 [t_V + \frac{1}{2} X_{xu}] \\
&+ \hat{Y}_{xu}^3 \hat{Y}_{xd} [- \frac{2M_S^2(2M_S^2 + M_V^2)}{3(M_S^2 + M_V^2)^2} - \frac{\tilde{A}_{xu}(2\tilde{A}_{xu} + \tilde{A}_{xd})}{3(M_S^2 + M_V^2)}] \\
&+ \hat{Y}_{xu}^2 \hat{Y}_{xd}^2 [- \frac{M_S^4}{(M_S^2 + M_V^2)^2} - \frac{(\tilde{A}_{xu} + \tilde{A}_{xd})^2}{3(M_S^2 + M_V^2)}] \\
&+ \hat{Y}_{xu} \hat{Y}_{xd}^3 [- \frac{2M_S^2(2M_S^2 + M_V^2)}{3(M_S^2 + M_V^2)^2} - \frac{\tilde{A}_{xd}(2\tilde{A}_{xd} + \tilde{A}_{xu})}{3(M_S^2 + M_V^2)}] \\
&+ \hat{Y}_{xd}^4 [t_V + \frac{1}{2} X_{xd}] \}, \qquad (5.6)
\end{aligned}
$$

where

$$
\begin{aligned}
&\hat{Y}_{xu} = Y_{xu} \sin\beta, \qquad \hat{Y}_{xd} = Y_{xd} \cos\beta, \qquad t_V = \log \frac{M_S^2 + M_V^2}{M_V^2}, \\
&X_{xu} = - \frac{2M_S^2(5M_S^2 + 4M_V^2) - 4(3M_S^2 + 2M_V^2)\tilde{A}_{xu}^2 + \tilde{A}_{xu}^4}{6(M_V^2 + M_S^2)^2}, \\
&X_{xd} = - \frac{2M_S^2(5M_S^2 + 4M_V^2) - 4(3M_S^2 + 2M_V^2)\tilde{A}_{xd}^2 + \tilde{A}_{xd}^4}{6(M_V^2 + M_S^2)^2}, \\
&\tilde{A}_{xu} = A_{xu} - \mu \cot\beta, \qquad \tilde{A}_{xd} = A_{xd} - \mu \tan\beta, \qquad (5.7)
\end{aligned}
$$

We set $Y_{XD} = 0$, $Y_{XU} = 1$, $A_{XD} = 0$, allow A_{XU} to run, and approximate M_S by $\sqrt{M_{\tilde{t}_1} M_{\tilde{t}_2}}$.

A better approximation would allow these flippon Yukawa and trilinear couplings to run.

Once we have allowed the couplings to run, we may allow the individual flippon masses to run.

We accomplish this by introducing the corrections to the renormalization group equations.

5.2.4 Below M_{32}

Corrections to existing β functions:

$$
\begin{aligned}
\Delta\beta_{\mu} &= \frac{\mu}{16\pi^2}(3Y_{XD}^2 + 3Y_{XU}^2), \\
\Delta\beta_{B_{\mu}} &= \frac{6}{16\pi^2}(Y_{XD}^2 A_{XD} + Y_{XU}^2 A_{XU}^2), \\
\Delta\beta_{Y_u} &= \frac{3Y_u Y_{XU}^2}{16\pi^2}, \\
\Delta\beta_{Y_d} &= \frac{3Y_d Y_{XD}^2}{16\pi^2}, \\
\Delta\beta_{Y_e} &= \frac{3Y_e Y_{Xd}^2}{16\pi^2}, \\
\Delta\beta_{A_u} &= \frac{6A_{XU} Y_{XU}^2}{16\pi^2}, \\
\Delta\beta_{A_d} &= \frac{6A_{XD} Y_{Xd}^2}{16\pi^2}, \\
\Delta\beta_{A_e} &= \frac{6A_{XD} Y_{Xd}^2}{16\pi^2}, \\
\Delta\beta_{M_{H_u}^2} &= \frac{6}{16\pi^2}(M_{H_u}^2 + \tilde{M}_{XQ^c}^2 + \tilde{M}_{XD}^2 + |A_{XU}|^2) Y_{XD}^2, \\
\Delta\beta_{M_{H_d}^2} &= \frac{6}{16\pi^2}(M_{H_d}^2 + \tilde{M}_{XQ}^2 + \tilde{M}_{XD^c}^2 + |A_{XD}|^2) Y_{XD}^2, \\
\Delta\beta_{v_u} &= \frac{-3Y_{XU}^2 v_u}{16\pi^2}, \\
\Delta\beta_{v_d} &= \frac{-3Y_{XD}^2 v_d}{16\pi^2}
\end{aligned}
\tag{5.8}
$$

And β functions for some of the most important of the new parameters:

$$
\begin{aligned}
\beta_{M_{XQ}} &= \frac{M_{XQ}}{16\pi^2}(Y_{XU}^2 + Y_{XD}^2 - \frac{16}{3}g_3^2 - 3g_2^2 - \frac{1}{15}g_1^2), \\
\beta_{M_{XD}} &= \frac{M_{XD}}{16\pi^2}(2Y_{XU}^2 + 2Y_{XD}^2 - \frac{16}{3}g_3^2 - \frac{4}{15}g_1^2), \\
\beta_{M_{XE}} &= \frac{-12M_{XE}g_1^2}{80\pi^2}, \\
\beta_{B_{XQ}} &= \frac{1}{16\pi^2}(2Y_{XU}^2 A_{XU} + 2Y_{XD}^2 A_{XD} + \frac{32}{3}g_3^2 M_3 + 6g_2^2 M_2 + \frac{2}{15}g_1^2 M_1), \\
\beta_{B_{XD}} &= \frac{1}{16\pi^2}(4Y_{XU}^2 A_{XU} + 4Y_{XD}^2 A_{XD} + \frac{32}{3}g_3^2 M_3 + \frac{8}{15}g_1^2 M_1), \\
\beta_{A_{XU}} &= \frac{1}{16\pi^2}(6Y_u^2 A_u + 12Y_{XU}^2 A_{XU} + \frac{32}{3}g_3^2 M_3 + 6g_2^2 M_2 + \frac{14}{15}g_1^2 M_1), \\
\beta_{A_{XD}} &= \frac{1}{16\pi^2}(6Y_d^2 A_d + 2Y_e^2 A_e + 12Y_{XD}^2 A_{XD} + \frac{32}{3}g_3^2 M_3 + 6g_2^2 M_2 + \frac{14}{15}g_1^2 M_1), \\
\beta_{\tilde{M}_{XQ}^2} &= \frac{1}{16\pi^2}(Y_{XD}^2(2\tilde{M}_{XQ}^2 + 2M_{H_d}^2 + \tilde{M}_{XD^c}^2 + 2|A_{XD}|^2) \\
&\quad -\frac{32}{3}g_3^2 M_3^2 - 6g_2^2 M_2^2 - \frac{2}{15}g_1^2 M_1^2 + \frac{1}{5}g_1^2 S), \\
\beta_{\tilde{M}_{XQ^c}^2} &= \frac{1}{16\pi^2}(Y_{XU}^2(2\tilde{M}_{XQ^c}^2 + 2M_{H_u}^2 + \tilde{M}_{XD}^2 + 2|A_{XU}|^2) \\
&\quad -\frac{32}{3}g_3^2 M_3^2 - 6g_2^2 M_2^2 - \frac{2}{15}g_1^2 M_1^2 + \frac{1}{5}g_1^2 S), \\
\beta_{\tilde{M}_{XD}^2} &= \frac{1}{16\pi^2}(Y_{XU}^2(4\tilde{M}_{XQ^c}^2 + 4M_{H_u}^2 + 4\tilde{M}_{XD}^2 + 4|A_{XU}|^2) \\
&\quad -\frac{32}{3}g_3^2 M_3^2 - \frac{8}{15}g_1^2 M_1^2 + \frac{2}{5}g_1^2 S), \\
\beta_{\tilde{M}_{XD^c}^2} &= \frac{1}{16\pi^2}(Y_{XD}^2(4\tilde{M}_{XQ}^2 + 4M_{H_d}^2 + 4\tilde{M}_{XD^c}^2 + 4|A_{XD}|^2) \\
&\quad -\frac{32}{3}g_3^2 M_3^2 - \frac{8}{15}g_1^2 M_1^2 + \frac{2}{5}g_1^2 S), \\
\beta_{\tilde{M}_{XE}^2} &= \frac{1}{16\pi^2}(\frac{-24}{5}g_1^2 M_1^2 + \frac{6}{5}g_1^2 S), \\
\beta_{\tilde{M}_{XE^c}^2} &= \frac{1}{16\pi^2}(\frac{-24}{5}g_1^2 M_1^2 + \frac{6}{5}g_1^2 S)
\end{aligned}
\tag{5.9}
$$

where

$$S = M_Z + \frac{1}{2}(\mu + \frac{M_1 + M_2 + M_3}{3}) + \tilde{M}^2_{XQ} + \tilde{M}^2_{XD} + \tilde{M}^2_{XE} + \tilde{M}^2_{XQ^c} + \tilde{M}^2_{XD^c} + \tilde{M}^2_{XE^c} \tag{5.10}$$

5.2.5 Above M_{32}

This energy region requires the most modification to existing code. Implementation of the partial unification is however, relatively straight forward given that the existing particles are grouped into multiplets. The flippon corrections are equally numerous, though. Again we have corrections to existing β functions:

$$
\begin{aligned}
\Delta\beta_{\lambda_1^b} &= \frac{1}{16\pi^2}\lambda_1^b 3Y_{XD}^2, \\
\Delta\beta_{\lambda_2^t} &= \frac{1}{16\pi^2}\lambda_2^t 3Y_{XU}^2, \\
\Delta\beta_{\lambda_3^\tau} &= \frac{1}{16\pi^2}\lambda_3^\tau 3Y_{XD}^2, \\
\Delta\beta_{\lambda_4} &= \frac{1}{16\pi^2}\lambda_4 3Y_{XD}^2, \\
\Delta\beta_{\lambda_5} &= \frac{1}{16\pi^2}\lambda_5 3Y_{XU}^2, \\
\Delta\beta_{A_b} &= 6A_{XD}Y_{XD}^2 \\
\Delta\beta_{A_t} &= 6A_{XU}Y_{XU}^2 \\
\Delta\beta_{A_\tau} &= 6A_{XD}Y_{XD}^2 \\
\Delta\beta_{A_4} &= 6A_{XD}Y_{XD}^2 \\
\Delta\beta_{A_5} &= 6A_{XU}Y_{XU}^2 \\
\Delta\beta_{\mu} &= \frac{1}{16\pi^2}\mu(3Y_{XU}^2 + 3Y_{XD}^2) \\
\Delta\beta_{B_\mu} &= \frac{6}{16\pi^2}(A_{XU}Y_{XU}^2 + A_{XD}Y_{XD}^2) \\
\Delta\beta_{v_u} &= \frac{-3v_u Y_{XU}^2}{16\pi^2} \\
\Delta\beta_{v_d} &= \frac{-3v_d Y_{XD}^2}{16\pi^2} \\
\Delta\beta_{M_h^2} &= \frac{6F_{XD}}{16\pi^2} \\
\Delta\beta_{M_{h^c}^2} &= \frac{6F_{XU}}{16\pi^2}
\end{aligned}
\tag{5.11}
$$

$$
\begin{aligned}
\beta_{Y_{XD}} &= \frac{Y_{XD}}{16\pi^2}(3(\lambda_1^b)^2 + (\lambda_3^\tau)^2 + 3(\lambda_4)^2 + 9Y_{XD}^2 - \frac{96}{5}g_5^2 - \frac{3}{10}g_{1X}^2), \\
\beta_{Y_{XU}} &= \frac{Y_{XU}}{16\pi^2}(4(\lambda_1^t)^2 + 3(\lambda_5)^2 + 9Y_{XU}^2 - \frac{96}{5}g_5^2 - \frac{3}{10}g_{1X}^2), \\
\beta_{A_{XD}} &= \frac{2}{16\pi^2}(3A_b(\lambda_1^b)^2 + A_\tau(\lambda_3^\tau)^2 + 3A_4\lambda_4^2 + 9A_{XD}Y_{XD}^2 + \frac{5}{96}g_5^2M_5 + \frac{3}{10}g_{1X}^2M_{1X}) \\
\beta_{A_{XU}} &= \frac{2}{16\pi^2}(4A_t(\lambda_2^t)^2 + 3A_5\lambda_5^2 + 9A_{XU}Y_{XU}^2 + \frac{5}{96}g_5^2M_5 + \frac{3}{10}g_{1X}^2M_{1X}), \\
\beta_{M_{XF}} &= \frac{M_{XF}}{16\pi^2}(Y_{XU}^2 + Y_{XD}^2 - \frac{72}{5}g_5^2 - \frac{1}{10}g_{1X}^2), \\
\beta_{M_{XE}} &= \frac{-5M_{XE}g_{1X}^2}{32\pi^2}, \\
\beta_{B_{XF}} &= \frac{2}{16\pi^2}(A_{XU}Y_{XU}^2 + A_{XD}Y_{XD}^2 + \frac{72}{5}g_5^2M_5 + \frac{1}{10}g_{1X}^2M_{1X}), \\
\beta_{B_{XE}} &= \frac{5g_{1X}^2M_{1X}}{16\pi^2}, \\
\beta_{\tilde{M}_{XF}^2} &= \frac{2}{16\pi^2}(3F_{XD} - \frac{72}{5}g_5^2M_5^2 - \frac{1}{10}g_{1X}^2M_{1X}^2), \\
\beta_{\tilde{M}_{\bar{X}F}^2} &= \frac{2}{16\pi^2}(3F_{XU} - \frac{72}{5}g_5^2M_5^2 - \frac{1}{10}g_{1X}^2M_{1X}^2), \\
\beta_{\tilde{M}_{XE}^2} &= \frac{-5g_{1X}^2M_{1X}^2}{16\pi^2}, \\
\beta_{\tilde{M}_{XE^c}^2} &= \frac{-5g_{1X}^2M_{1X}^2}{16\pi^2},
\end{aligned}
\tag{5.12}
$$

Where

$$
\begin{aligned}
F_{XD} &\equiv Y_{XD}^2(2\tilde{M}_{XF}^2 + M_h^2 + A_{XD}^2), \\
F_{XU} &\equiv Y_{XU}^2(2\tilde{M}_{\bar{X}F}^2 + M_{\bar{h}}^2 + A_{XU}^2).
\end{aligned}
\tag{5.13}
$$

We require that the flippon terms also respect the NSS boundary conditions. In

practical terms, we also require low scale boundary conditions because that is how the algorithm begins. We require that for each flippon term, the boundary conditions are copies of the corresponding third generation SM term. In addition, top quark radiative corrections are required in order to keep the flippon Yukawa couplings finite.

6. NATURALNESS IN F-SU(5)

6.1 Naturalness in Other Models

SuSpect [10] provides a subroutine to calculate the finetuning with respect to μ. In order to set the scale for our expectations, we consider a few mSUGRA points where the gluino mass, stop masses, and μ are similar to in our benchmark models, as well as depend in a similar way on $M_{1/2}$ as in our models. The results of that are presented in figure 6.1.

Baer et. al. in [9] introduce Δ_{EW} in an attempt to let correlations between high scale parameters cancel out through the running of the RGEs down to the weak scale. They consider a variety of models. The mSUGRA/CMSSM model had $(\Delta_{EW})_{min} \sim 100$ in the hyperbolic or focal point region where μ may be minimized. The Non-Universal Higgs Model 1 obtains $(\Delta_{EW})_{min} \sim 30$ where the radiative corrections $\Sigma_u^u(\tilde{t})$ provides the limiting factor. This is improved in a similar model, NUHM2 with $(\Delta_{EW})_{min} \sim 10$, in that paper. A minimum of 7 was reported in [8]. This low value is reached through large squark mixing which limits the effects of the radiative corrections. Minimal Gauge Mediated Supersymmetry Breaking has $(\Delta_{EW})_{min} \sim 1000$, where consistency with LHC measurements of M_h requires heavy messenger scale giving heavy squarks, and thus significant radiative corrections. The Minimal Anomaly Mediated Supersymmetry Breaking model requires several TeV scale stops to be consistent with the LHC Higgs mass, resulting in $(\Delta_{EW})_{min} \sim 100$. The string-derived Hypercharge-AMSB has $(\Delta_{EW})_{min} \sim 100$.

The Moduli-Anomaly Mediated Supersymmetry Breaking model displays a variety of behaviors depending on the modular weights of the matter and higgs fields. Both types of modular weight can take a value of 0, 1/2, and 1. For $n_H = 0$, $n_m = 0$

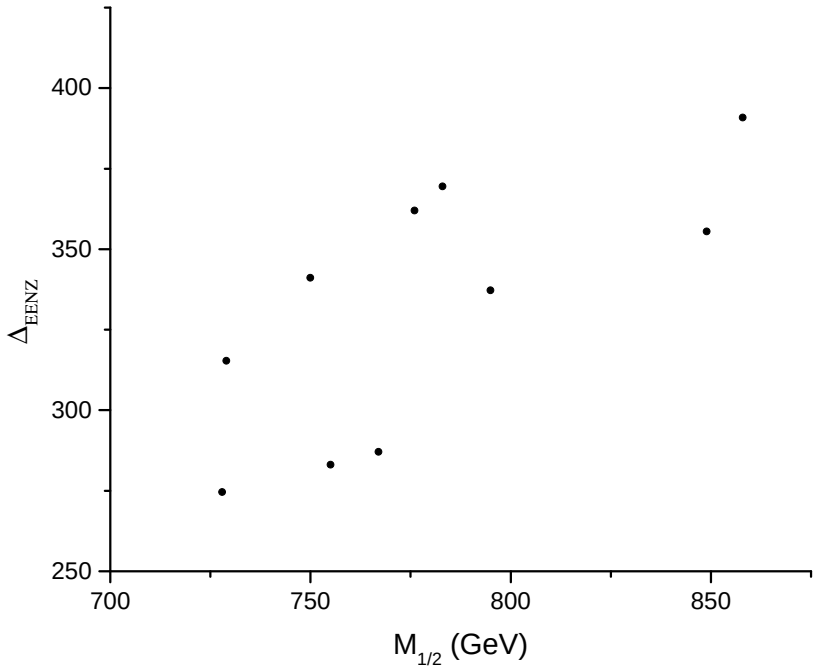

Figure 6.1: Δ_{EENZ} as calculated by the SuSpect finetuning subroutine for mSUGRA. The points have been chosen to match up with the range of the gluino mass, stop masses, and μ in $\mathcal{F}$-SU5, as well has having similar dependence on $M_{1/2}$.

has $(\Delta_{EW})_{min} \sim 437$ with large gaugino masses and large μ. Less fine tuned regions are inconsistent with the LHC Higgs mass. $n_H = 0$, $n_m = 1/2$ has $(\Delta_{EW})_{min} \sim 314$, with the lower fine tuned regions violating rare B-decays. $n_H = 0$, $n_m = 1$ has $(\Delta_{EW})_{min} \sim 91$ constrained by radiative corrections. For $n_H = 1/2$, $n_m = 0$, $(\Delta_{EW})_{min} \sim 457$, $n_H = 1/2$, $n_m = 1/2$, $(\Delta_{EW})_{min} \sim 375$, and $n_H = 1/2$, $n_m = 1$, $n_H = 1/2$, $n_m = 1/2$, $(\Delta_{EW})_{min} \sim 100$, all are due to a relatively heavy spectrum. The same situation holds for the $n_H = 1$ case, with $(\Delta_{EW})_{min}$ ranging from 859 to 1643.

6.2 Naturalness in $\mathcal{F}$-SU(5)

We will utilize the Giudice-Masiero mechanism [31] to solve the μ problem in our model. We allow the Kähler modulus T to generate an F term which will give an effective

$$\mu = \langle F_T \rangle / M_{Pl}$$

From this, we obtain $\mu = cM_{1/2}$, where c is an $\mathcal{O}(1)$ constant which must be determined by iterated running of the RGEs.

Using SuSpect [10], the renormalization group equations are run from M_Z up to M_F using a fourth order Runge-Kutta method with adaptive step sizes. Since this $\mathcal{F}$-theory construction only applies locally, we remain ignorant of the full Kähler potential, particularly for the SM fermions and Higgs fields. However, we may start from the simplest No Scale SUGRA assumption, using this to derive the soft SUSY breaking terms at M_F. The high energy boundary conditions ($M_0 = A_0 = B_\mu = 0$, $M_{1/2} \neq 0$) are then applied and the equations are run down to the electroweak symmetry breaking (EWSB) scale and then M_Z. The equations are run back up to M_F to calculate $\mu(M_F)$, among other quantities, and this procedure is repeated until

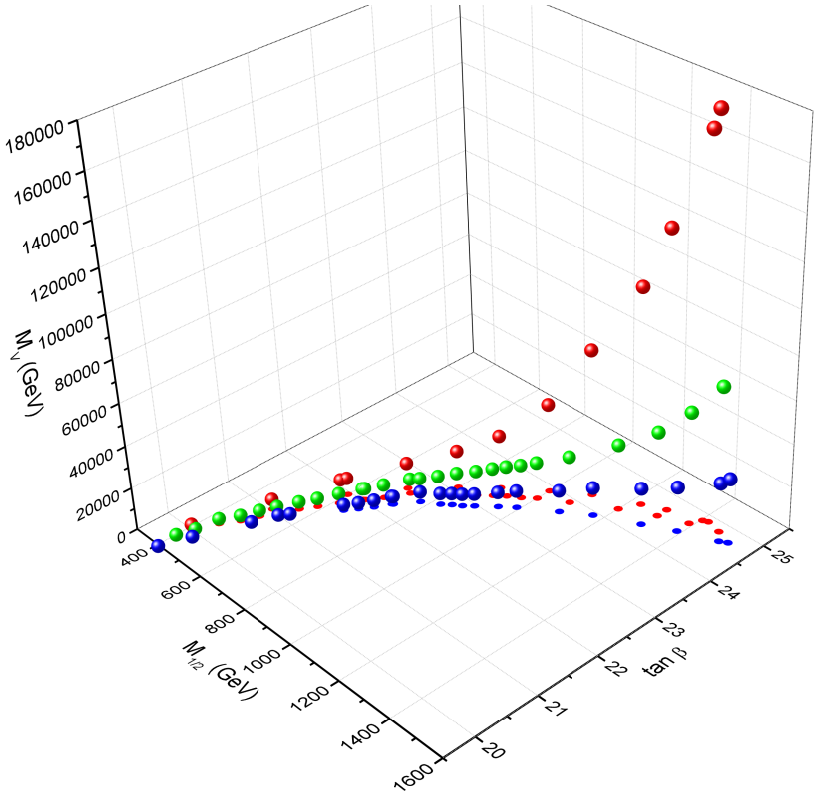

Figure 6.2: The benchmark points in our parameter space. The projection on the $\tan\beta$-$M_{1/2}$ is almost independent of M_{top} while M_V is strongly dependent upon M_{top} and $M_{/2}$. $M_{top} = 173.3$ GeV is indicated in green, $M_{top} = 174.4$ GeV is indicated in red, $M_{top} = 172.2$ GeV is indicated in blue.

the equations converge to a solution. If the equations do converge, then the mass spectrum is calculated and many of the known experimental constraints mentioned in the previous chapter may be applied.

After applying the experimental constraints we are left with an essentially one dimensional subspace of our parameter space after removing the dependence upon M_{top} as illustrated in figure 6.2.

Since our model has only one free parameter, the finetuning of the model should be easy to calculate. A standard means of comparison has been the effect of parameters on M_Z [32]. In general, for a set of parameters a_i in a model, we define:

$$c_i = \frac{\partial \log M_Z^2}{\partial a_i}$$

A model is finetuned with respect to a parameter a_i if c_i is large. There is room for subjectivity, but this allows a quantitative measure of finetuning with which we may compare the amount of finetuning for different models. Since we do not care if a model is very natural with respect to one parameter while it is extremely finetuned with respect to another, we shall define:

$$\Delta_{EENZ} = max\{c_i\}$$

If we simply consider the tree level result from the MSSM for M_Z:

$$\frac{1}{2}M_Z^2 = \frac{M_{H_d}^2}{\tan^2\beta - 1} - \frac{\tan^2\beta M_{H_u}^2}{\tan^2\beta - 1} - \mu^2 \tag{6.1}$$

we see that for the moderately large values of $\tan\beta$ that are favored by our model, we may approximate M_Z by:

$$\frac{1}{2}M_Z^2 \approx -M_{H_u}^2 - \mu^2 \tag{6.2}$$

If we include radiative corrections, Σ_u^u and Σ_d^d as done by Baer et. al. [8], we instead get

$$\frac{1}{2}M_Z^2 = \frac{M_{H_d}^2 + \Sigma_d^d}{\tan^2\beta - 1} - \frac{\tan^2\beta(M_{H_u}^2 + \Sigma_u^u)}{\tan^2\beta - 1} - \mu^2 \tag{6.3}$$

However, given that the contributions from the radiative corrections are at least an order of magnitude smaller than those at tree level, we may safely ignore them for the moment.

The correlations between the parameters that we put into SuSpect and our actual parameter in our model force us to conclude that the finetuning subroutine built into SuSpect provides an overestimate, much as claimed by Baer et. al. [8]. The first effort at estimating the finetuning involved treating M_Z as an input parameter for the model and allowing small variations around the true value. We suspect that this result was unreliable because many of the SuSpect functions and subroutines have a subtle and hardcoded dependence upon $M_Z = 91.187GeV$. These results tended to give a result for $\partial M_Z/\partial M_{1/2}$ between 0.001 and 0.005. A less direct, though ultimately simpler, method relied on the cornucopia of experimental constraints to restrict the model to only one effective parameter. These constraints include $M_Z = 91.187GeV$, so the dependence of the right hand side of 6.1 on $M_{1/2}$ will change as we change $M_{1/2}$. Thus we can evaluate the finetuning of an individual point in our parameter space, but we cannot get a closed form expression for $\Delta_{EENZ}(M_{1/2})$. Using equation 6.1 with single parameter $M_{1/2}$ and treating $\tan\beta$ as a constant, we get:

$$\frac{\partial \log M_Z^2}{\partial \log M_{1/2}^2} = \frac{2M_{1/2}^2}{M_Z^2}\left(\frac{\frac{\partial M_{H_d}^2}{\partial M_{1/2}^2} - \tan^2\beta \frac{\partial M_{H_u}^2}{\partial M_{1/2}^2}}{\tan^2\beta - 1} - \frac{\partial \mu^2}{\partial M_{1/2}^2}\right) \tag{6.4}$$

This gives us a good first approximation, the results of which are shown in figure 6.3.

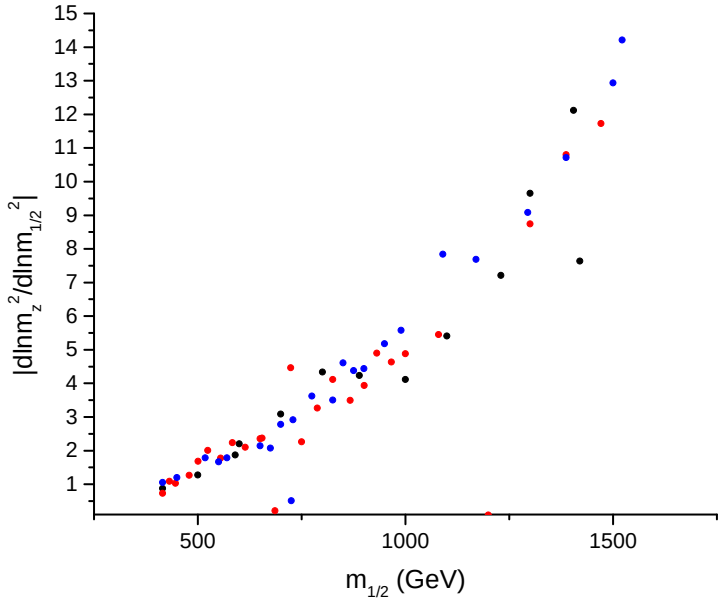

Figure 6.3: The first approximation of Δ_{EENZ} as a function of $m_{1/2}$. Radiative corrections are not included, and $\tan\beta$ is taken as fixed for each benchmark point. The top quark mass is allowed to vary, $M_{top} = 172.2$ GeV is indicated in black, $M_{top} = 173.3$ GeV is indicated in red, $M_{top} = 174.4$ GeV is indicated in blue.

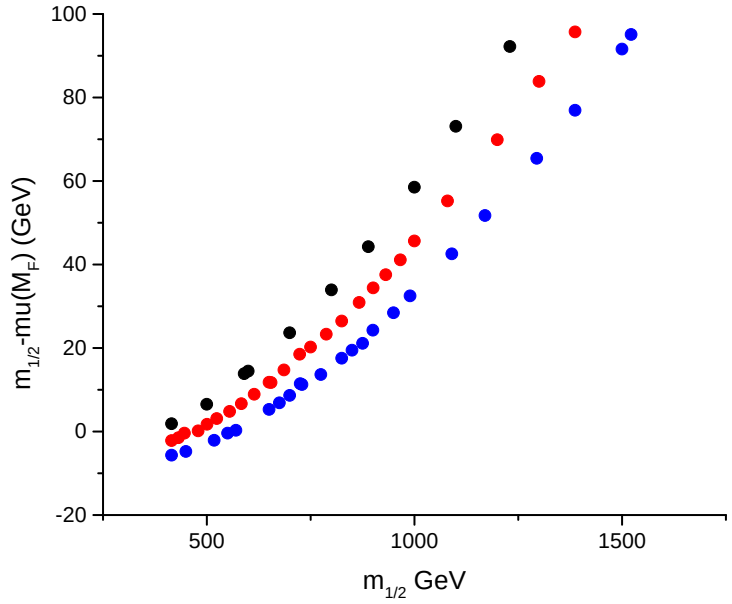

Figure 6.4: $m_{1/2} - \mu(M_F)$ as a function of $m_{1/2}$. The top quark mass is allowed to vary, $m_{top} = 172.2$ GeV is indicated in black, $m_{top} = 173.3$ GeV is indicated in red, $m_{top} = 174.4$ GeV is indicated in blue.

Already we see one of the prominent characteristics of our model. The finetuning becomes more pronounced as we increase $M_{1/2}$. This also corresponds to an increasing difference between μ and $M_{1/2}$, as shown in figure 6.4.

As a next approximation, we can include the dependence of $\tan\beta$ on $M_{1/2}$,

$$\begin{aligned}\frac{\partial \log M_Z^2}{\partial \log M_{1/2}^2} &= \frac{2M_{1/2}^2}{M_Z^2}\Big(\frac{\frac{\partial M_{H_d}^2}{\partial M_{1/2}^2} - \tan^2\beta \frac{\partial M_{H_u}^2}{\partial M_{1/2}^2}}{\tan^2\beta - 1} - \frac{\partial \mu^2}{\partial M_{1/2}^2} \\ &\quad + 2\tan\beta \frac{\partial \tan\beta}{\partial M_{1/2}^2}\Big(\frac{M_{H_u}^2}{\tan^2\beta - 1} - \frac{M_{H_d}^2 - \tan^2\beta M_{H_u}^2}{(\tan^2\beta - 1)^2}\Big) \qquad (6.5)\end{aligned}$$

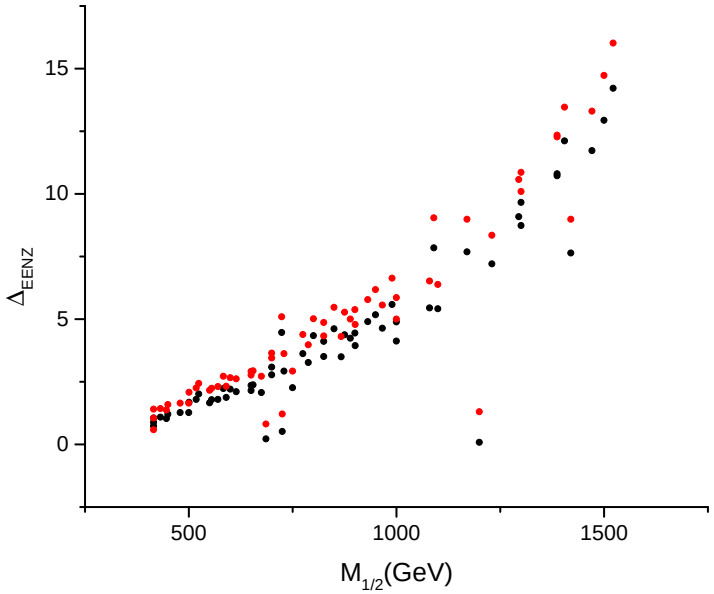

Figure 6.5: Δ_{EENZ} for all benchmark points with dependence on $\tan\beta$ (red) and without (black). This still excludes radiative corrections.

For low $M_{1/2}$, this has a relatively dramatic effect, but overall including the variation of $\tan\beta$ with $M_{1/2}$ provides a slightly larger, though still extraordinarily small, finetuning as shown in figure 6.5.

Including the radiative corrections to M_Z from [33] we get

$$\frac{1}{2}M_Z^2 = \frac{M_{H_d}^2 + \Sigma_d^d}{\tan^2\beta - 1} - \frac{\tan^2\beta(M_{H_u}^2 + \Sigma_u^u)}{\tan^2\beta - 1} - \mu^2 \tag{6.6}$$

Again, because of the large value of our $\tan\beta$, we can focus on the up contributions. The dominant radiative correction is from the stops.

$$
\begin{aligned}
\Sigma_u^u(\tilde{t}_{1,2}) &= \frac{3}{16\pi^2} F(M^2_{\tilde{t}_{1,2}})(f_t^2 - g_Z^2 \mp \frac{f_t^2 A_t^2 - 8g_Z^2(\frac{1}{4} - \frac{2}{3}x_W)\Delta_t}{M^2_{\tilde{t}_2} - M^2_{\tilde{t}_1}}) \\
\Sigma_u^u(\tilde{b}_{1,2}) &= \frac{3}{16\pi^2} F(M^2_{\tilde{b}_{1,2}})(g_Z^2 \mp \frac{f_b^2\mu^2 + 8g_Z^2(\frac{1}{4} - \frac{1}{3}x_W)\Delta_b}{M^2_{\tilde{b}_2} - M^2_{\tilde{b}_1}}) \\
\Sigma_u^u(\tilde{\tau}_{1,2}) &= \frac{1}{16\pi^2} F(M^2_{\tilde{b}_{1,2}})(g_Z^2 \mp \frac{f_b^2\mu^2 + 8g_Z^2(\frac{1}{4} - x_W)\Delta_b}{M^2_{\tilde{b}_2} - M^2_{\tilde{b}_1}}) \\
\Sigma_u^u(\tilde{u}_L) &= \frac{3}{16\pi^2} F(M^2_{\tilde{u}_L})(f_u^2 - 4g_Z^2(\frac{1}{2} - \frac{2}{3}x_W)) \\
\Sigma_u^u(\tilde{u}_R) &= \frac{3}{16\pi^2} F(M^2_{\tilde{u}_R})(f_u^2 - 4g_Z^2(\frac{2}{3}x_W)) \\
\Sigma_u^u(\tilde{W}^{\pm}_{1,2}) &= \frac{-g^2}{16\pi^2} F(M^2_{\tilde{W}_{1,2}}))(1/mp \frac{M_2^2 + \mu^2 - 2M_W^2 \cos 2\beta}{M^2_{W_2} - M^2_{W_1}}) \\
\Sigma_u^u(\tilde{Z}_i) &= \frac{1}{16\pi^2} \frac{F(M^2_{\tilde{Z}_i})}{D(\tilde{Z}_i)} (K(\tilde{Z}_i) - 2(g^2 + g'^2)\mu^2 M_Z^2 \cos^2\beta (M^2_{\tilde{Z}_i} - M^2_{\tilde{\gamma}})) \\
\Sigma_u^u(W^{\pm}) &= \frac{3g^2}{16\pi^2} F(M_W^2) \\
\Sigma_u^u(Z) &= \frac{3g^2}{64\pi^2 \cos^2\theta_W} F(M_Z^2) \\
\Sigma_u^u(h, H) &= \frac{g_Z^2}{16\pi^2} F(M^2_{h,H})(1 \mp \frac{M_Z^2 + M_A^2(1 + 4\cos 2\beta + 2\cos^2 2\beta)}{M_H^2 - M_h^2}) \\
\Sigma_u^u(H^{\pm}) &= \frac{g^2}{32\pi^2} F(M^2_{H^{\pm}}) \\
\Sigma_u^u(t) &= -\frac{3f_t^2}{8\pi^2} F(M_t^2) \\
\Sigma_u^u(b) &= 0 \\
\Sigma_u^u(\tau) &= 0
\end{aligned}
\tag{6.7}
$$

For completeness, the radiative contributions to the down Higgs mass are:

$$
\begin{aligned}
\Sigma_d^d(\tilde{t}_{1,2}) &= \frac{3}{16\pi^2}F(M^2_{\tilde{t}_{1,2}})(g_Z^2 \mp \frac{f_t^2\mu^2 + 8g_Z^2(\frac{1}{4}-\frac{2}{3}x_W)\Delta_t}{M^2_{\tilde{t}_2}-M^2_{\tilde{t}_1}}) \\
\Sigma_d^d(\tilde{b}_{1,2}) &= \frac{3}{16\pi^2}F(M^2_{\tilde{b}_{1,2}})(f_b^2 - g_Z^2 \mp \frac{f_b^2A_b^2 - 8g_Z^2(\frac{1}{4}-\frac{1}{3}x_W)\Delta_b}{M^2_{\tilde{b}_2}-M^2_{\tilde{b}_1}}) \\
\Sigma_d^d(\tilde{\tau}_{1,2}) &= \frac{1}{16\pi^2}F(M^2_{\tilde{b}_{1,2}})(f_b^2 - g_Z^2 \mp \frac{f_b^2A_b^2 - 8g_Z^2(\frac{1}{4}-x_W)\Delta_b}{M^2_{\tilde{b}_2}-M^2_{\tilde{b}_1}}) \\
\Sigma_d^d(\tilde{u}_L) &= \frac{3}{16\pi^2}F(M^2_{\tilde{u}_L})(4g_Z^2(\frac{1}{2}-\frac{2}{3}x_W)) \\
\Sigma_d^d(\tilde{u}_R) &= \frac{3}{16\pi^2}F(M^2_{\tilde{u}_R})(4g_Z^2(\frac{2}{3}x_W)) \\
\Sigma_d^d(\tilde{W}^{\pm}_{1,2}) &= \frac{-g^2}{16\pi^2}F(M^2_{\tilde{W}_{1,2}}))(1 \mp \frac{M_2^2+\mu^2+2M_W^2\cos 2\beta}{M^2_{W_2}-M^2_{W_1}}) \\
\Sigma_d^d(\tilde{Z}_i) &= \frac{1}{16\pi^2}\frac{F(M^2_{\tilde{Z}_i})}{D(\tilde{Z}_i)}(K(\tilde{Z}_i) - 2(g^2+g'^2)\mu^2M_Z^2\sin^2\beta(M^2_{\tilde{Z}_i}-M^2_{\tilde{\gamma}})) \\
\Sigma_d^d(W^{\pm}) &= \frac{3g^2}{16\pi^2}F(M_W^2) \\
\Sigma_d^d(Z) &= \frac{3g^2}{64\pi^2\cos^2\theta_W}F(M_Z^2) \\
\Sigma_d^d(h,H) &= \frac{g_Z^2}{16\pi^2}F(M^2_{h,H})(1 \mp \frac{M_Z^2+M_A^2(1-4\cos 2\beta+2\cos^2 2\beta)}{M_H^2-M_h^2}) \\
\Sigma_d^d(H^{\pm}) &= \frac{g^2}{32\pi^2}F(M^2_{H^{\pm}}) \\
\Sigma_d^d(t) &= 0 \\
\Sigma_d^d(b) &= -\frac{3f_b^2}{8\pi^2}F(M_b^2) \\
\Sigma_d^d(\tau) &= -\frac{f_\tau^2}{8\pi^2}F(M_\tau^2)
\end{aligned}
\tag{6.8}
$$

where for brevity we have

$$g_Z^2 = \frac{g^2 + g'^2}{8}$$

$$F(M^2) = M^2(\log \frac{M^2}{M_{\tilde{t}_1} M_{\tilde{t}_2}} - 1)$$

$$D(\tilde{Z}_i) = \prod_{j \neq i} (M^2_{\tilde{Z}_i} - M^2_{\tilde{Z}_j})$$

$$K(\tilde{Z}_i) = -M^6_{\tilde{Z}_i}(g^2 + g'^2)$$

$$+M^4_{\tilde{Z}_i}(g^2(M_1^2 + \mu^2) + g'^2(M_2^2 + \mu^2) + M_Z^2(g^2 + g'^2)$$

$$-M^2_{\tilde{Z}_i}(\mu^2(g^2 M_1^2 + g'^2 M_2^2) + (g^2 + g'^2) M_Z^2 M^2_{\tilde{\gamma}}))$$

$$M_{\tilde{\gamma}} = M_1 \cos^2 \theta_W + M_2 \sin^2 \theta_W$$

$$\Delta_t = (M^2_{\tilde{t}_L} - M^2_{\tilde{t}_R})/2 + M_Z^2 \cos 2\beta (\frac{1}{4} - \frac{2}{3} x_W)$$

$$\Delta_b = (M^2_{\tilde{b}_L} - M^2_{\tilde{b}_R})/2 + M_Z^2 \cos 2\beta (\frac{1}{4} - \frac{2}{3} x_W)$$

6.3 Why?

A first indication of why the $\mathcal{F}$-SU(5) theory is so natural may be obtained by seeing how the various constraints we have imposed relate to one another.

Upon allowing M_Z to vary with a fixed M_V, we find an exact correlation between $M_{1/2}$ and $\mu(M_F)$.

Relaxing the $B_\mu(M_F) = 0$ condition, and floating M_Z, we find $\mu = M_{1/2}$ only for M_Z between approximately 89.4 GeV and 91.6 GeV as shown in figure 6.6.

In particular, we shall see that the $B_\mu = 0$ condition strongly constrains the mass of the Z boson in our model. Thus, we have enveloped the weak scale finetuning issue in a symmetry of our boundary conditions. Conversely, considering only three currently known masses, M_{top}, M_Z, and M_h, we immediately arrive in our model at the relation $\mu(EWSB) = M_{1/2}$, and thus the Higgs mass is giving us a very large

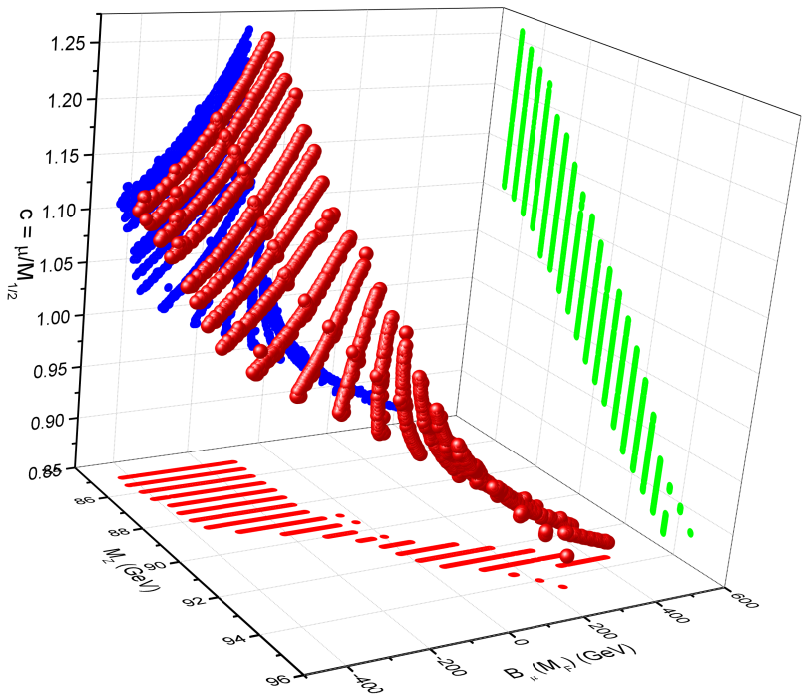

Figure 6.6: Requiring only that the RGE's do not produce any errors and additionally allowing M_Z to float, we can see how our solutions would react to loosening of the various low and high scale boundary conditions. Here $M_{1/2}$ is allowed to vary between 230 GeV and 1.5 TeV, $\tan\beta$ varied between 20 and 24.4, M_V varied between 4700 GeV and 7624 GeV, while M_{top} was kept constant at 173.3 GeV.

hint about our high energy boundary conditions.

7. DILATON-MODULI MEDIATED SUSY BREAKING MODEL

As an alternative to the successful and natural model mentioned in the previous chapters, we may instead consider an M-theory derived dilaton-moduli mediated SUSY breaking model. M-theory may be considered as another strongly coupled limit of type IIB string theory. In particular, we wish to compactify M-theory on an $S_1/\mathbb{Z}_2$ orbifold. This will allow each E_8 gauge group to live on the singularities of the orbifold, giving a natural separation between the observable sector and the hidden sector. The dilaton and moduli will then mediate SUSY breaking from the hidden sector, through the bulk, to the observable sector. We want to break the E_8 group down to the SM in the observable sector, but in the hidden sector, we can leave E_8 unbroken, or break it to various subgroups. This hidden sector group will have a slight effect on the soft SUSY breaking masses in their dependence upon the quadratic Casimir operator of the hidden sector group.

This model has only three parameters, $M_{3/2}$, $\tan\beta$, and a parameterization of the mixing between dilaton and moduli fields x. This mixing is dependent upon the hidden sector coupling strength α_H.

Assuming unified gaugino masses $M_{1/2}$, scalar masses M_0, and trilinear couplings A_0, we obtain the following results from Li [34] assuming vanishing cosmological constant:

$$
\begin{aligned}
M_{1/2} &= \frac{\sqrt{3}M_{3/2}}{1+x}(\sin\theta + \frac{x}{\sqrt{3}}\cos\theta) \\
M_0^2 &= M_{3/2}^2 - \frac{3M_{3/2}^2}{(3+x)^2}(x(6+x)\sin^2\theta + (3+2x)\cos^2\theta - 2\sqrt{3}x\sin\theta\cos\theta) \\
A_0 &= -\frac{\sqrt{3}M_{3/2}^2}{3+x}((3-2x)\sin\theta + \sqrt{3}x\cos\theta)
\end{aligned} \tag{7.1}
$$

where for convenient parameterization we have:

$$
\begin{aligned}
x &= \frac{\alpha_H - \alpha_{GUT}}{\alpha_H + \alpha_{GUT}} \\
\tan\theta &= \frac{1}{\sqrt{3}} \frac{\alpha_{GUT} + \frac{2\pi}{C_2(\mathcal{G}_{hidden})}\frac{2}{1+x}}{\alpha_{GUT} - \frac{2\pi}{3C_2(\mathcal{G}_{hidden})}\frac{2\pi}{1+x}}
\end{aligned} \tag{7.2}
$$

The parameter space was scanned using DarkSUSY [35]. Much of the work was done with $\tan\beta = 35$, in which case the gravitino mass acted as an overall scaling and the hidden sector coupling strength (recast as x) acts as a tilting angle between M_0 and $M_{1/2}$ as shown in figure 7.1. The only part of the parameter space that was consistant with the dark matter relic density was in the coannihilation region, this is shown in figure 7.1. The coannihilation region is the strip of parameter space where the LSP and the stau are very close in mass, allowing the reaction $\chi_1^0\tilde{\tau} \to ff$ in addition to $\chi_1^0\chi_1^0 \to ff$. This extra annihilation channel allows the dark matter relic density to be brought down to observed levels.

Upon obtaining a reduced parameter space that satisfies the experimental constraints known at the time (namely excluding the Higgs mass), the MadGraph [36] [37] suite was used to begin LHC event simulation. The Madgraph suite includes utilizes MadEvent to generate parton-level events, these are then taken as input

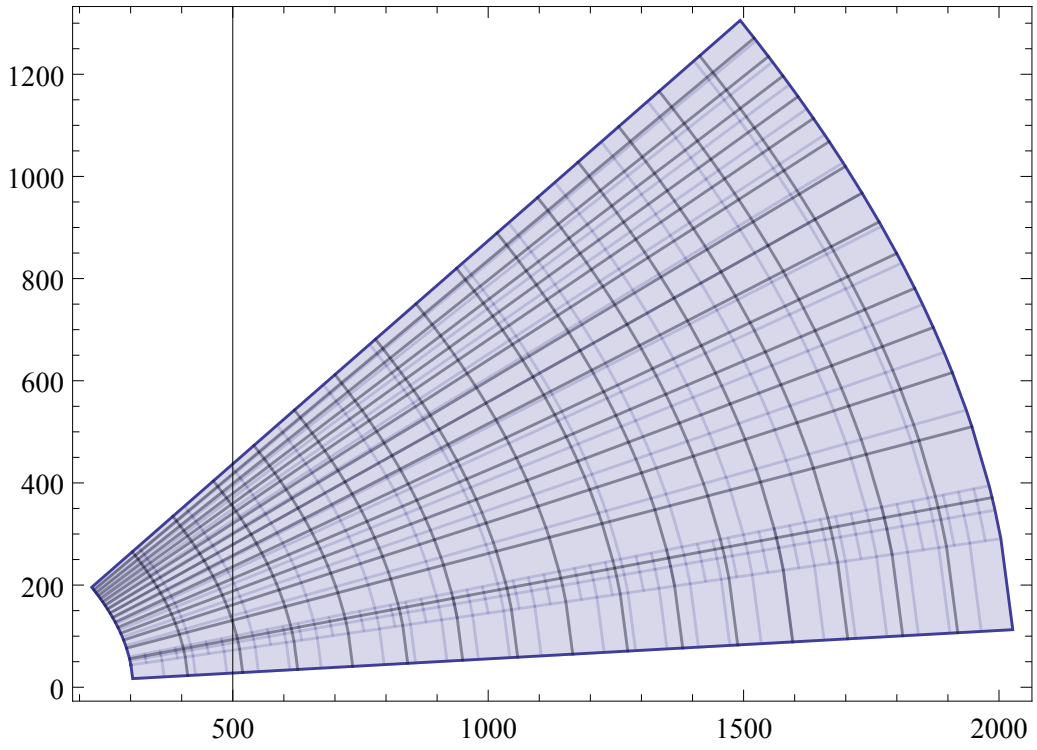

Figure 7.1: M_0 vs $M_{1/2}$ for $M_{3/2}$ between 200 GeV and 2 TeV and x between .625 and 1, both axes are in GeV

to Pythia to move to hadron-level, which is then fed into PGS with LHC detector cards to simulate the detectors. A script to cut events by Walker [38] was used to remove background events. Before LHC signatures could be found, the discovery of the Higgs mass at around 126 GeV motivated a return to looking at the allowed parameter space of the model to try to satisfy that constraint.

As a first step, the restriction on the dark matter relic density was relaxed to an upper limit. The tension between the Higgs mass and the dark matter relic density continued to eliminate the total parameter space. Next, non-universal gaugino masses from untwisted (0,2) Abelian orbifolds were considered.

Following [39] we obtain:

$$\begin{aligned}
\frac{M_0^2}{M_{3/2}^2} &= 1 + 3\cos^2\theta(n_1\sin^2\alpha\sin^2\beta + n_2\sin^2\alpha\cos^2\beta + n_3\cos^2\alpha) \\
\frac{M_a}{M_{3/2}} &= \frac{\sqrt{3}}{Re(f_a)}(k_a Re(S)\sin\theta + \cos\theta\sum_{i=1}^{3}\frac{b_a'^i - k_a\delta_{GS}^i}{\sqrt{1-a_i}}\Theta_i 2\frac{Re(T_i)}{32\pi^2}(\frac{-4\pi}{\eta(T_i)}\frac{d\eta(T_i)}{dT_i} - \frac{\pi}{Re(T_i)}))
\end{aligned} \tag{7.3}$$

where

$$\begin{aligned}
a_i &= \frac{\delta_{GS}^i}{24\pi^2(Re(S) - \sum_{i=1}^{3}\frac{\delta_{GS}^i}{8\pi^2}\log Re(T_i))} \\
b_a'^i &= -C(\mathcal{G}_a) + \sum_{reps}\frac{C(R_a)Dim(R_a)}{Dim(R_a)}(1+2n^i) \\
\delta_{GS}^i &= 15 - 30\frac{ord(\mathcal{N}=2)_i}{ord(\mathcal{G}_{orbifold})}
\end{aligned} \tag{7.4}$$

Not all combinations of orbifold moduli spaces and modular weights are allowed. For $h_{1,1} = 3$, $h_{1,2} \in (0, 1, 3)$, the orbifold modululi space is $(\frac{SU(1,1)}{U(1)})_T^3 \times (\frac{SU(1,1)}{U(1)})_U^{h_{2,1}}$, and $\mathrm{K} = -\sum_{i=1}^{3} \log Re(T_i) - \sum_{m=1}^{h_{2,1}} \log Re(U_m)$. For $h_{2,1} = 0$, allowed orbifolds are $\mathbb{Z}_7$, $\mathbb{Z}_8'$,$\mathbb{Z}_8'$,$\mathbb{Z}_6' \times \mathbb{Z}_2$,$\mathbb{Z}_6' \times \mathbb{Z}_2$,$\mathbb{Z}_6' \times \mathbb{Z}_2$. For $h_{2,1} = 1$, allowed orbifolds are $\mathbb{Z}_6$,$\mathbb{Z}_6$,$\mathbb{Z}_8$,$\mathbb{Z}_4 \times \mathbb{Z}_2$,$\mathbb{Z}_6 \times \mathbb{Z}_2$,$\mathbb{Z}_{12}'$. For $h_{2,1} = 3$ the only allowed orbifold is $\mathbb{Z}_2 \times \mathbb{Z}_2$. For $h_{1,1} = 5$, $h_{1,2} \in (0, 1)$, the orbifold moduli space is $(\frac{SU(1,1)}{U(1)} \bigotimes \frac{SU(2,2)}{SU(2)\times SU(2)\times U(1)})_T \bigotimes (\frac{SU(1,1)}{U(1)})_U^{h_{2,1}}$, and $\mathrm{K} = -\log Re(T_1) - \log\det Re(T_{ij}) - \sum_{m=1}^{h_{2,1}} \log Re(U_m)$. The only allowed orbifold for $h_{2,1} = 0$ is $\mathbb{Z}_6'$ and for $h_{2,1} = 1$ is $\mathbb{Z}_4$. For $h_{1,1} = 9$, $h_{2,1} = 1$, the orbifold moduli space is $(\frac{SU(3,3)}{SU(3)\times SU(2)\times U(1)})_T$, $\mathrm{K} = -\log\det Re(T_{ij})$, and the orbifold is $\mathbb{Z}_3$. However, generically, this parameter space was too large to effectively scan.

The universal model would have been another candidate for the finetuning analysis as presented in the previous chapter except for its unfortunate contradiction with experimental data. A non-universal extension of that model might evade the experimental constraints, but it is our conclusion that even in the best case scenario, such a model would be an over-fitting of available data. Any useful physical insight would be hiding within the vast parameter space which itself is just a way of expressing our ignorance of the high energy theory.

8. CONCLUSION

The $\mathcal{F}$-SU(5) model has demonstrated robust success against experimental constraints while retaining strong theoretical assumptions. It incorporates the particle content, solutions to standard GUT problems, and sub-Planckian group structure of older F-SU(5) models, the strong assumptions and tree-level vanishing of the cosmological constant of No Scale Supergravity, and takes its inspiration from $\mathcal{F}$-theory, and so promises a stringy ultraviolet completion. It has survived the current experimental constraints and has a spectrum within the reach of the 14 TeV LHC.

These current experimental constraints cut down the parameter space to an extent that the entire model may be effectively treated with a single parameter. This single parameter naturally leads to large correlations between SUSY breaking terms at the EWSB scale. The cancellation between terms because of this correlation in turn leads to minimal finetuning in this model. Specifically, the similar dependence of M_{H_u} and μ upon $M_{1/2}$ lead to natural cancellations, even for large values of those (low-scale) parameters. This close cancellation, as opposed to M_{H_u} and μ each being arbitrary functions of $M_{1/2}$ may be traced to the high scale boundary condition $B_\mu = 0$, thus allowing a symmetry from our No Scale SUGRA boundary conditions to absorb the complicated issue of electroweak finetuning.

A natural next step is to investigate the effects of the radiative corrections more completely. Another goal is to approximate closed form expressions for the terms in 6.6 in terms of $M_{1/2}$. Full implementation of flippon corrections to RGEs has yet to be implemented. Finally, a more analytic understanding of the effects of the boundary conditions on low energy quantities would provide immense insight.

REFERENCES

[1] Tianjun Li, James A. Maxin, Dimitri V. Nanopoulos, and Joel W. Walker. The Golden Point of No-Scale and No-Parameter $\mathcal{F}$-$SU(5)$, arXiv:1007.5100. *Phys.Rev.*, D83:056015, 2011.

[2] Tianjun Li, James A. Maxin, Dimitri V. Nanopoulos, and Joel W. Walker. A Higgs Mass Shift to 125 GeV and A Multi-Jet Supersymmetry Signal: Miracle of the Flippons at the $\sqrt{s} = 7$ TeV LHC, arXiv:1112.3024. *Phys.Lett.*, B710:207–214, 2012.

[3] Tianjun Li, James A. Maxin, Dimitri V. Nanopoulos, and Joel W. Walker. The Race for Supersymmetric Dark Matter at XENON100 and the LHC: Stringy Correlations from No-Scale F-SU(5), arXiv:1106.1165. *JHEP*, 1212:017, 2012.

[4] Tianjun Li, James A. Maxin, Dimitri V. Nanopoulos, and Joel W. Walker. No-Scale F-SU(5) in the Light of LHC, Planck and XENON, arXiv:1305.1846. *J.Phys.*, G40:115002, 2013.

[5] Tianjun Li, James A. Maxin, Dimitri V. Nanopoulos, and Joel W. Walker. One-Parameter Model for the Superworld, arXiv:1210.8043. 2012.

[6] Jonathan J. Heckman and Cumrun Vafa. From F-theory GUTs to the LHC, arXiv:0809.3452. 2008.

[7] H. Baer and X. Tata. *Weak Scale Supersymmetry: From Superfields to Scattering Events*. Cambridge University Press, Cambridge, UK, 2006.

[8] Howard Baer, Vernon Barger, and Dan Mickelson. How conventional measures overestimate electroweak fine-tuning in supersymmetric theory, arXiv:1309.2984. *Phys.Rev.*, D88:095013, 2013.

[9] Howard Baer, Vernon Barger, Dan Mickelson, and Maren Padeffke-Kirkland. SUSY models under siege: LHC constraints and electroweak fine-tuning, arXiv:1404.2277. 2014.

[10] Abdelhak Djouadi, Jean-Loic Kneur, and Gilbert Moultaka. SuSpect: A Fortran code for the supersymmetric and Higgs particle spectrum in the MSSM, arXiv:hep-ph/0211331. *Comput.Phys.Commun.*, 176:426–455, 2007.

[11] Zvi Bern, Lance J. Dixon, and Radu Roiban. Is N = 8 supergravity ultraviolet finite?, arXiv:hep-th/0611086. *Phys.Lett.*, B644:265–271, 2007.

[12] M. Kaku. *Quantum field theory: A Modern introduction.* Oxford University Press, Oxford, UK, 1993.

[13] P. Binetruy. *Supersymmetry: Theory, experiment and cosmology.* Cambridge University Press, Cambridge, UK, 2006.

[14] P.A.R. Ade et al. Planck 2013 results. XVI. Cosmological parameters, arXiv:1303.5076. 2013.

[15] R. Agnese et al. Silicon Detector Dark Matter Results from the Final Exposure of CDMS II, arXiv:1304.4279. *Phys.Rev.Lett.*, 111:251301, 2013.

[16] E. Aprile et al. Dark Matter Results from 225 Live Days of XENON100 Data, arXiv:1207.5988. *Phys.Rev.Lett.*, 109:181301, 2012.

[17] D.S. Akerib et al. First results from the LUX dark matter experiment at the Sanford Underground Research Facility, arXiv:1310.8214. 2013.

[18] Christoph Weniger. A Tentative Gamma-Ray Line from Dark Matter Annihilation at the Fermi Large Area Telescope, arXiv:1204.2797. *JCAP*, 1208:007, 2012.

[19] Torsten Bringmann, Xiaoyuan Huang, Alejandro Ibarra, Stefan Vogl, and Christoph Weniger. Fermi LAT Search for Internal Bremsstrahlung Signatures from Dark Matter Annihilation, arXiv:1203.1312. *JCAP*, 1207:054, 2012.

[20] ATLAS Collaboration. Observation of an excess of events in the search for the Standard Model Higgs boson in the gamma-gamma channel with the ATLAS detector, CERN Document Server: ATLAS-CONF-2012-091, ATLAS-COM-CONF-2012-109. 2012.

[21] Serguei Chatrchyan et al. Observation of a new boson at a mass of 125 GeV with the CMS experiment at the LHC, arXiv:1207.7235. *Phys.Lett.*, B716:30–61, 2012.

[22] G.W. Bennett et al. Measurement of the negative muon anomalous magnetic moment to 0.7 ppm, arXiv:hep-ex/0401008. *Phys.Rev.Lett.*, 92:161802, 2004.

[23] S. Chen et al. Branching fraction and photon energy spectrum for b to s gamma, arXiv:hep-ex/0108032. *Phys.Rev.Lett.*, 87:251807, 2001.

[24] Bernard Aubert et al. Measurement of the B to X(s) gamma branching fraction and photon energy spectrum using the recoil method, arXiv:0711.4889. *Phys.Rev.*, D77:051103, 2008.

[25] A. Limosani et al. Measurement of Inclusive Radiative B-meson Decays with a Photon Energy Threshold of 1.7-GeV, arXiv:0907.1384. *Phys.Rev.Lett.*, 103:241801, 2009.

[26] R. Aaij et al. Measurement of the $B_s^0 \to \mu^+\mu^-$ branching fraction and search for $B^0 \to \mu^+\mu^-$ decays at the LHCb experiment, arXiv:1307.5024. *Phys.Rev.Lett.*, 111:101805, 2013.

[27] Tianjun Li, James A. Maxin, Dimitri V. Nanopoulos, and Joel W. Walker. Has SUSY Gone Undetected in 9-jet Events? A Ten-Fold Enhancement in the LHC Signal Efficiency, arXiv:1108.5169. 2011.

[28] J.P. Derendinger, Jihn E. Kim, and Dimitri V. Nanopoulos. Anti-SU(5). *Phys.Lett.*, B139:170, 1984.

[29] Jing Jiang, Tianjun Li, Dimitri V. Nanopoulos, and Dan Xie. Flipped SU(5) x U(1)(X) Models from F-Theory, arXiv:0905.3394. *Nucl.Phys.*, B830:195–220, 2010.

[30] Yunjie Huo, Tianjun Li, Dimitri V. Nanopoulos, and Chunli Tong. The Lightest CP-Even Higgs Boson Mass in the Testable Flipped $SU(5) \times U(1)_X$ Models from F-Theory, arXiv:1109.2329. *Phys.Rev.*, D85:116002, 2012.

[31] G.F. Giudice and A. Masiero. A Natural Solution to the mu Problem in Supergravity Theories. *Phys.Lett.*, B206:480–484, 1988.

[32] John R. Ellis, K. Enqvist, Dimitri V. Nanopoulos, and F. Zwirner. Observables in Low-Energy Superstring Models. *Mod.Phys.Lett.*, A1:57, 1986.

[33] Howard Baer, Vernon Barger, Peisi Huang, Dan Mickelson, Azar Mustafayev, et al. Radiative natural supersymmetry: Reconciling electroweak fine-tuning and the Higgs boson mass, arXiv:1212.2655. *Phys.Rev.*, D87(11):115028, 2013.

[34] Tian-jun Li. Soft terms in M theory, arXiv:hep-ph/9804243. *Phys.Rev.*, D59:107902, 1999.

[35] P. Gondolo, J. Edsjo, P. Ullio, L. Bergstrom, Mia Schelke, et al. DarkSUSY: Computing supersymmetric dark matter properties numerically, arXiv:astro-ph/0406204. *JCAP*, 0407:008, 2004.

[36] Johan Alwall, Pavel Demin, Simon de Visscher, Rikkert Frederix, Michel Herquet, et al. MadGraph/MadEvent v4: The New Web Generation, arXiv:0706.2334. *JHEP*, 0709:028, 2007.

[37] Johan Alwall, Michel Herquet, Fabio Maltoni, Olivier Mattelaer, and Tim Stelzer. MadGraph 5 : Going Beyond, arXiv:1106.0522. *JHEP*, 1106:128, 2011.

[38] Joel W. Walker. CutLHCO: A Consumer-Level Tool for Implementing Generic Collider Data Selection Cuts in the Search for New Physics, arXiv:1207.3383. 2012.

[39] Tatsuo Kobayashi, Daijiro Suematsu, Kiyonori Yamada, and Yoshio Yamagishi. Nonuniversal soft scalar masses in superstring theories, arXiv:hep-ph/9408322. *Phys.Lett.*, B348:402–410, 1995.